uOttawa

L'Université canadienne
Canada's university

FACULTÉ DES ÉTUDES SUPÉRIEURES ET POSTOCTORALES

uOttawa

L'Université canadienne
Canada's university

FACULTY OF GRADUATE AND POSDOCTORAL STUDIES

Sha Wang

AUTEUR DE LA THÈSE / AUTHOR OF THESIS

M.A.Sc. (Electrical Engineering)

GRADE / DEGREE

School of Information Technology and Engineering

FACULTÉ, ÉCOLE, DÉPARTEMENT / FACULTY, SCHOOL, DEPARTMENT

Video Quality Measurement using Digital Watermaking

TITRE DE LA THÈSE / TITLE OF THESIS

J. Zhao

DIRECTEUR (DIRECTRICE) DE LA THÈSE / THESIS SUPERVISOR

CO-DIRECTEUR (CO-DIRECTRICE) DE LA THÈSE / THESIS CO-SUPERVISOR

EXAMINATEURS (EXAMINATRICES) DE LA THÈSE / THESIS EXAMINERS

A. Cuhadar

R. Laganière

Gary W. Slater

LE DOYEN DE LA FACULTÉ DES ÉTUDES SUPÉRIEURES ET POSTDOCTORALES /
DEAN OF THE FACULTY OF GRADUATE AND POSTDOCORAL STUDIES

Video Quality Measurement using Digital Watermarking

by

Sha Wang

A thesis submitted to the University of Ottawa in partial fulfillment of the requirements for the degree of M.A.Sc

Ottawa-Carleton Institute for Electrical and Computer Engineering
School of Information Technology and Engineering
University of Ottawa

Ottawa, Ontario, Canada

September 2005

Your file Votre référence
ISBN: 0-494-11450-9
Our file Notre référence
ISBN: 0-494-11450-9

Abstract

A 3-level DWT (Discrete Wavelet Transform) based objective video quality measurement method is proposed based on semi-fragile digital watermarking. The watermark is embedded into the luminance components of the Intra frames of an MPEG-2 video stream, which can be treated as images. The degradation of the watermark is used to estimate the degradation of the cover work. A quantization method is used to embed the watermark. In the watermark embedding process, 10 quantization parameters are assigned to the 10 DWT decomposed blocks which are obtained by applying 3-level DWT to the target image. And the watermark is embedded with its vulnerability adjusted according to the different frequency distribution of the content of the cover work. Automatic control is used to adjust the watermark vulnerability which is controlled by the watermark bit portions and the quantization parameters. By referring to the ideal mapping curve which is the pre-calculated relationship between the quality in terms of the classical metrics and the True Detection Rates (TDR), the TDR and quality measurement (PSNR/wPSNR/Watson JND) relationship curve of any test image can be converged to the ideal mapping curve so that the quality of the degraded image can easily measured by checking the ideal mapping curve with the TDR computed during the watermark extraction. The TDR is calculated between the original watermark and the degraded watermark. After the watermark extraction, the degradation of the extracted watermark is used to estimate video/image quality in terms of the classical metrics. By comparing the video quality estimated by the proposed method with the calculated quality in terms of PSNR, wPSNR, and JND, it is clear that the proposed method can be used to evaluate video quality against compression with high accuracy.

Contents

List of Tables

List of Figures

List of Acronyms

CSF	Contrast Sensitivity Function
DCT	Discrete Cosine Transform
DWT	Discrete Wavelet Transform
FFT	Fast Fourier Transform
GOP	Group of Pictures
HAS	Human Auditory System
HVS	Human Visual System
IDWT	Inverse Discrete Wavelet Transform
JND	Just Noticeable Distance
JPEG	Joint Photographic Experts Group
MPEG	Moving Picture Experts Group
MSE	Mean Square Error
NVF	Noise Visibility Function
PSNR	Peak Signal to Noise Ratio
TDR	Truly Detected Rates
wPSNR	weighted Peak Signal to Noise Ratio

This thesis is dedicated to my parents, Aunt Su and Uncle Kao.

Acknowledgement

I would like to thank my supervisor, Professor Jiying Zhao, for bringing the problem of digital watermarking to me, and for his patient guidance and feedback during every step of my work.

I also would like to thank Dong Zheng for his valuable advice and help.

And I deeply appreciate the encouragement and financial supports from my parents, Aunt Su and Uncle Kao.

Chapter 1

Introduction

1.1 Digital watermarking

With the rapid development of digital techniques, we have seen an explosion of data exchange in the Internet and the extensive use of digital media. Consequently, this leads to the problem of illegal copying and redistribution of digital information. The roles of digital watermarking were highly noticed when the needs of content authentication and copyright protection increased urgently. Digital watermarking is a kind of technique to imperceptibly insert additional information into the image/video through slight modification of the data. For different purposes, the additional information, which is also called digital watermark, can be embedded into the image/video robustly or fragilely and will undergo the same distortions as the cover work. The retrieved digital watermark serves multiple purposes, such as the proof of the ownership and copyright, the indication of the possible content tampering.

1.1.1 A typical watermarking system and watermark classifications

A typical watermarking system is essentially composed of watermark embedding process and watermark extraction process which can be expressed using Fig. 1.1.

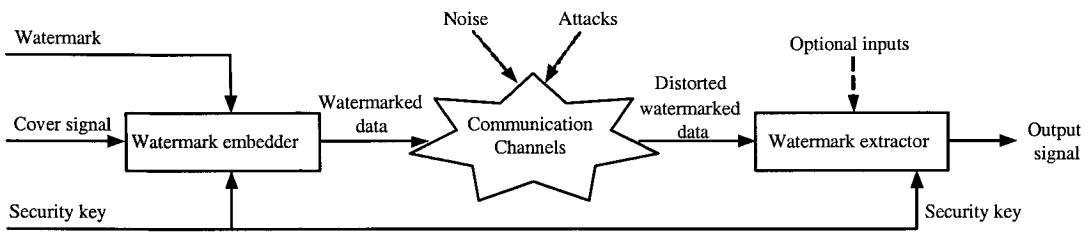

Figure 1.1: A digital watermarking system

The key components of Fig. 1.1 are: a watermark W, cover signal C, a security key K, watermarked data C_w, distorted watermarked data C'_w, output signal O, watermark embedder $e(\cdot)$ and watermark extractor $d(\cdot)$.

In the watermark embedding process, the inputs are the cover signal, watermark and a pre-set security key. The cover signal is the target image/video which can be an image, video, audio or other media expressions. For serving different purposes, the watermark can be a grey-scale image, a binary pattern or a number sequence, meaningful or random. The security key has a one-to-one correspondence with the watermark and is used to enhance the security of the entire system. As the output of the watermark embedder, the watermarked data might be changed by various intentional or unintentional attacks during its transmission. From a mathematical view, the watermark embedding process can also be expressed as:

$$C_w = e(C, W, K) \tag{1.1}$$

In the watermark extraction part, the watermark can be extracted with or without the access to the original cover signal C, and original watermark W. The extracted watermark can serve different purposes. The same security key as the one used in watermark embedding is applied to the watermark detection to ensure the success of watermark extraction. And the watermark extraction procedure can be depicted as follows:

$$O = d(C'_w, K, \cdots) \tag{1.2}$$

where C and W are always treated as the optional inputs for the watermark detector.

For a typical watermarking system, several requirements should be satisfied:

1. The watermark can be extracted from C_w or C'_w with or without the explicit knowledge of C.

2. C_w should be as close to C as possible.

3. If there are no distortions in data transmission, namely $C_w = C'_w$, the extracted watermark, W', should exactly match the original watermark, W.

Watermark can be generally categorized as in Fig. 1.2.

The visible watermark, which plays a less important role than the invisible watermark, is the one that is partially transparently placed over the content of image/video and can be hardly removed without damaging the cover works.

To work without affecting much to the image/video quality, digital watermark is usually designed to be completely invisible. And it can be classified as robust watermark, semi-fragile watermark and fragile watermark. The robust watermark can

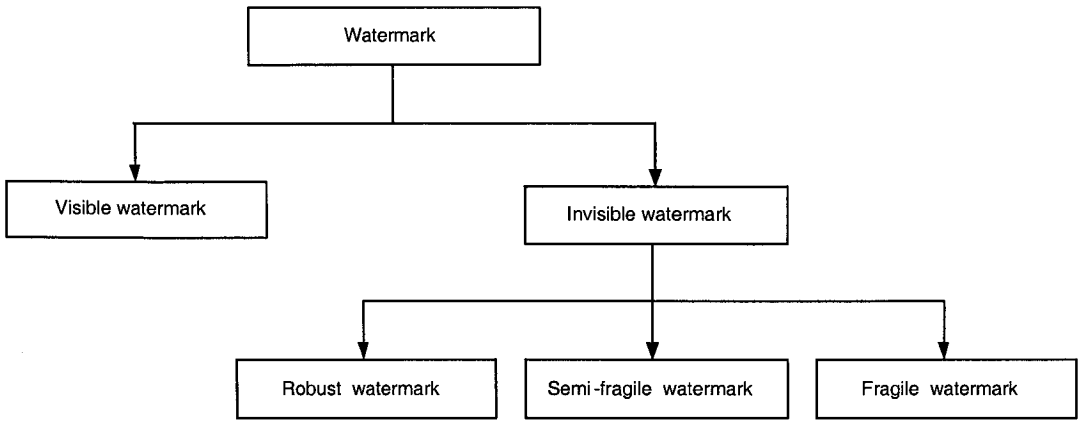

Figure 1.2: Watermark classifications

survive a vast amount of the intentional or unintentional attacks, which means the embedded watermark should be detectable even the host media data is severely distorted by those attacks, which is very popular in copyright protection [1][2][3]. The fragile watermark is used to monitor even the smallest alteration to its carrier in the application of content authentication [4]. And the semi-fragile watermark is designed to survive legitimate distortions to the cover works but be destroyed by illegitimate distortions, which recently have been proposed in quality evaluation of image/video [5][6][7][9][10].

Several kinds of popular watermarking techniques exist to provide choices to watermarking researchers: watermark is to be embedded in spatial domain or frequency domain of the image/video; watermark is to be embedded uniformly [7] or obeying some special properties like HVS (human visual system) [8]. To watermark some cover work, one way is to directly change the pixel values of the cover signal in the spatial domain. It is the simplest method while also the easiest way to get the watermark removed with one example method: pixel-wise forgery attack. More advanced techniques are to insert watermarks into some cover works in their transform domain using the well known transforms: FFT, DCT or DWT. On the other hand, the watermark can be

embedded uniformly without considering influences that watermarking might cause to the visual effects, or embedded according to HVS models with the aim of optimizing the watermarking techniques. Providing that a HVS threshold is not exceeded during the watermark embedding processes, the modified watermarked image/video will be undistinguishable to the human eye compared with the original one.

A simple example of watermark embedding can be illustrated using Fig. 1.3. The watermark is linearly embedded into the original image. α here is used to control the embedding strength. In this example, α equals to 1. The PSNR of the watermarked work is 48.59 dB.

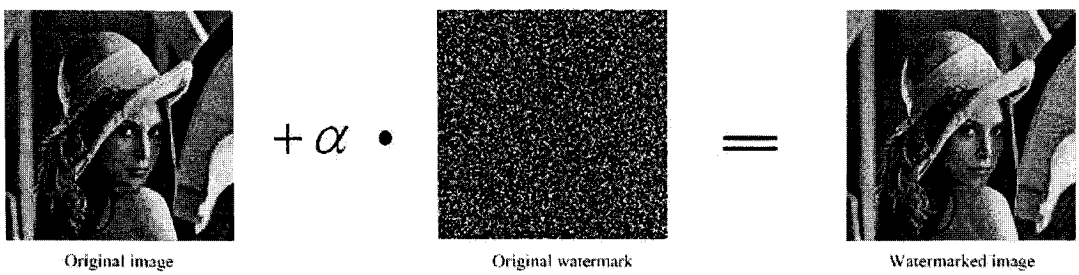

Figure 1.3: A simple example of watermark embedding

1.1.2 Main applications of digital watermarking

Among many others, the following are the main applications of digital watermarking.

1. Copyright protection

   The problem of copyright protection comes with the fast-growing illegitimate redistribution of image/video. In this application, the watermark, which carries the owner's copyright information, is robustly embedded into the image/video invisibly. And, even with serious distortions to the watermarked image/video,

the extracted watermark should still match the original watermark well to be able to give a clear judgment of the existence of the watermark.

2. Proof of ownership

   A further step from copyright protection for the watermarking technique is to prove ownership. The watermark should be unambiguous. The ambiguity attack is to embed additional watermark to claim to be the owner. The watermark used as a proof of ownership should be able to resolve the problem of the rightful ownership.

3. Content authentication

   The purpose of this application is to tell whether the content has been changed and fragile watermark contributes most to this application. Because the fragile watermark is likely to become undetectable after its cover work is modified, it is possible to monitor even the slightest changes or tampering to the content. Among all possible watermarking applications, authentication watermarks require lowest level of robustness.

4. Quality evaluation

   The semi-fragile watermark is used for media content quality evaluation. The watermark is embedded throughout the cover work with suitable vulnerabilities, so that the degradation of the watermark can reflect the degradation of the content quality of the host media. The watermarking metric should be able to not only tell whether the host media content has been tampered, but also evaluate the quality change of the host media content according to the characteristics of human visual/auditory system.

5. Broadcast monitoring

   The watermarks are embedded into the cover works in order to help the advertisers to identify when and where their works are broadcasted by recognizing watermarks embedded in the cover works.

6. Copy control

   The watermark exists to prevent people from illegally copying the copyrighted content.

1.2 Video watermarking

There exist several types of digital watermarking techniques with respect to different cover works, such as digital image watermarking, digital video watermarking, digital audio watermarking and 3D virtual objects watermarking. Among them, digital image watermarking has earned lots of attention during the past decade due to the availability of the images in digital format on the World Wide Web. And all of the watermarking applications have been realized for image watermarking. A further step from image watermarking is video watermarking.

For video watermarking, digital watermark can be embedded into video in its spatial domain or temporal domain [15][16][17][18]. Video may exist as raw video or compressed video. Raw video can be treated as a set of still images. So the image watermarking techniques can be applied to raw video. For the transmission convenience, video can be compressed into different formats using H.261, H.263, MPEG-1, MPEG-2, MPEG-4 etc. Being widely used in digital communications, MPEG-2 standard was considerably broader in scope and of wider appeal since it fixes many of the problems inherent

in MPEG-1 standard, such as scalability, handling of interlaced video and providing pictures with higher quality (studio quality and up to HDTV levels), and makes the digital transmission more economical [21]. Aware of the drawback of H.261, three types of frames were defined in MPEG-2, namely Intra frame (I), Predictive frame (P) and Bidirectional predictive frame (B), where I frame is a picture in absolute form carrying almost all the main information needed by the current Group of Picture (GOP) and can thoroughly determine the success or failure of encoding or decoding. And as the carriers of the prediction errors, P frame and B frame are found to be more sensitive to attacks, even small changes, than I frames. So, for different purposes of protection, it will be much better to embed watermark in temporal domain or I frames in spatial domain.

Because video has a huge embedding capability to carry as much additional information as possible, we can embed several watermarks into the video with each watermark serving its own purpose. Or, we can select embedding areas across all the GOPs according to some rules to realize one application.

In this thesis, we will mainly focus on MPEG-2 compressed video watermarking.

1.3 Quality evaluation metrics

Over the last few years, several objective/subjective image/video quality metrics are widely used, like mean square error (MSE), peak-signal-to-noise ratio (PSNR), weighted peak-signal-to-noise ratio (wPSNR) and Watson model. All of the existing quality metrics can be classified into two categories: objective quality metrics and subjective quality metrics.

1.3.1 Objective quality metrics

Objective quality metric is to measure the similarity between the distorted work and the original work. For the objective quality measurements, high quality means the distorted work is very similar to the original work. And low quality means the distorted work is much distinguishable from the original one. Such metrics include the widely-used mean squared error (MSE) and peak signal-to-noise ratio (PSNR). These measures are simple and easy to realize automated quality evaluations.

MSE is defined as:

$$MSE = \frac{1}{N}\Sigma(x_i - y_i)^2 \tag{1.3}$$

where, x_i and y_i respectively are the pixel values of the original work and the degraded work. N is the number of pixels in the current cover work.

And PSNR is defined as:

$$PSNR = 10\log_{10}\frac{L^2}{MSE} \tag{1.4}$$

where N is the number of pixels in the current cover work, L is the dynamic range. For an 8 bits/pixel grey-scale image, L is equal to 255.

1.3.2 Subjective quality metrics

The objective metrics always give us the over-estimated or under-estimated quality evaluations because of the ignorance of the specialty of human perception mechanisms. Sometimes, changes to the video/image negligible to the human eyes/ears can cause a dramatic difference of MSE or PSNR value. From the definitions of MSE and PSNR,

we can find that they treat the variations in all kinds of cover works equally. While, we know from the human perception mechanisms that all components of a cover work may not be equally perceptible. The human visual system has some well known features such as luminance masking, contrast sensitivity function, spatial/temporal frequency analysis and pooling. And the responses of the human auditory system can be affected much by the signal frequency and loudness.

To well measure the perceptual variations of video/image, many subjective quality metrics were proposed. The weighted PSNR (wPSNR) and Watson model are two frequently used subjective metrics.

1.3.2.1 wPSNR

As an MSE-based metric, wPSNR exists as an extension of the traditional PSNR to estimate the possible quality loss with taking part of the subjective factors into account. It works well by weighting each term of the PSNR using a local "activity" factor which is linked to the contrast sensitivity of the human vision, and becomes closer to perception than PSNR.

In the paper [22], Makoto Miyahara et al. proposed to model the spatial frequency response of the contrast sensitivity function (CSF) as follows:

$$CSF(f) = 2.6(0.0192 + 0.114f)e^{-0.114f^{1.1}} \tag{1.5}$$

where $f = \sqrt{u^2 + v^2}$, u and v are the horizontal and vertical frequency. To give a more accurate modelling, it has been proposed in [22] to further attenuate high frequency components with the following weighting factor.

$$O(f,\theta) = \frac{1 + e^{\beta(f-f_0)}\cos^4(2\theta)}{1 + e^{\beta(f-f_0)}} \tag{1.6}$$

where $\theta = \tan^{-1}(v/u)$ is the angle with respect to the vertical axis and horizontal axis in cycles/degree, and $\beta = 8$, $f_0 = 11.13$ *cycles/degree*. Thus,

$$CSF(f,\theta) = CSF(f)O(f,\theta) \tag{1.7}$$

To give an illustration of the contrast sensitivity function, CSF is drawn along the horizontal axis in Fig. 1.4. It is clear that the CSF is a low pass filter.

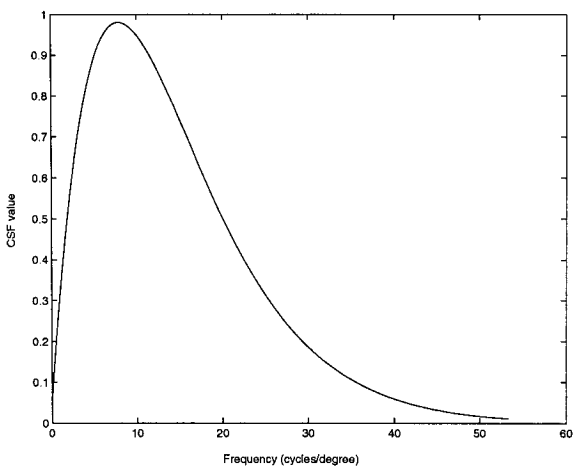

Figure 1.4: Contrast sensitivity function, $CSF(f)$

1.3.2.2 Watson model

Watson model [24] assesses the image visual quality by estimating the multiples of just noticeable differences (JNDs) between the original work and the distorted work. According to the mechanism of the human visual system, three factors are considered in the Watson model in order to more closely approximate the perceptual quality of

an image/video signal. And the three factors are: a frequency sensitivity function, a luminance masking function and a contrast masking function. Meanwhile, a pool component is used to combine all the estimated local perceptual distances together to achieve a global perceptual distance. The Watson model is designed in block DCT domain to accommodate to the image JPEG compression process.

1. The frequency sensitivity function

   The frequency sensitivity function estimates the human visual thresholds for one JND's distortion. It is derived in [32] utilizing a number of parameters, such as the distance between the viewer and the image and resolution of the image. For one 8 by 8 DCT block, one threshold is estimated for one coefficient. That means if the current coefficient is changed by the amount of its threshold, the distortion caused by this change may reach one JND. And an example set of thresholds for a DCT block can be illustrated using Fig. 1.5. In the figure, axis x and y respectively indicate the coefficients' horizontal and vertical indices in a block. The axis z represent the threshold values of the coefficients. The coordinate, $(0,0)$, in the figure corresponds to the DC component of the current DCT block. The smaller thresholds in the sensitivity map indicate that the human eyes are more sensitive to the changes of the components on these frequency components.

2. The luminance masking function

   The luminance masking function estimates the luminance masking thresholds for the block DCT coefficients. For a DCT block, if the intensity of its DC component is brighter, the block will be much more tolerant to changes. According the Watson model, the luminance masking thresholds for a DCT block can be adjusted using Equ. (1.8).

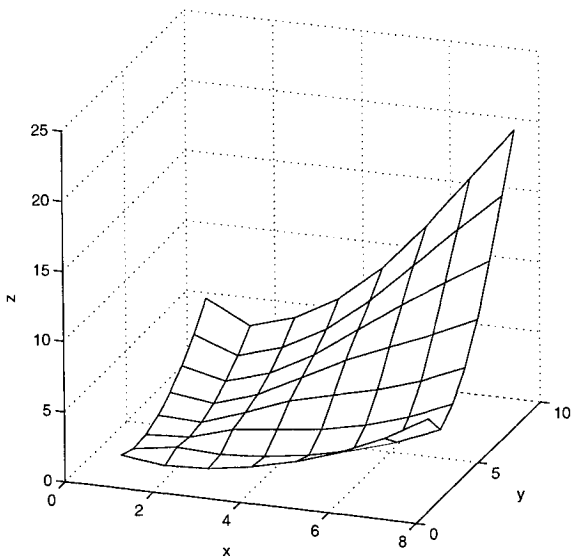

Figure 1.5: A frequency sensitivity threshold map

$$t_L(i,j,k) = t(i,j)(C_o(0,0,k)/C_{0,0})^{0.649} \tag{1.8}$$

where, t, $C_o(0,0,k)$, i and j are respectively the frequency sensitivity threshold map, the DC component, the line and column of a coefficient of the k^{th} DCT block, $C_{0,0}$ is the average value of the DC components in the image. The constant 0.649 is a suggested value that bridges the frequency sensitivity thresholds to the luminance masking thresholds.

3. The contrast masking function

   For the same DCT block, the contrast masking thresholds can be achieved using Equ. (1.9).

$$s(i,j,k) = max\{t_L(i,j,k), |C_o(i,j,k)|^{0.7} t_L(i,j,k)^{0.3}\} \tag{1.9}$$

The contrast masking thresholds are derived utilizing the frequency sensitivity thresholds and the luminance masking thresholds. For one DCT coefficient, it is a comprehensive threshold that indicates how many changes can be applied to the current frequency component while not being notified.

Thus, the Watson distance can be obtained by pooling all the local perceptual distances together using Equ. (1.11).

$$d(i,j,k) = \frac{e(i,j,k)}{s(i,j,k)} \tag{1.10}$$

$$D_{wat}(c_o, c_w) = (\sum_{i,j,k} |d(i,j,k)|^4)^{\frac{1}{4}} \tag{1.11}$$

where, d is the local perceptual distance, e is the differences between the original image and the distorted image in block DCT domain, and $D_{wat}(c_o, c_w)$ is the estimated Watson distance expressed as multiples of JNDs between the original image and the distorted image.

1.3.3 A watermarking-based quality metric

The MSE, PSNR, wPSNR, Watson model are widely used for quality evaluations of image/video, while all of these metrics are based on point-to-point calculation between the original work and the degraded work in spatial domain or frequency domain, which makes the access to the original work necessary. Sometimes, this will result in big inconveniences to the receiver side when the original work is a huge data packet, like video, or when it is real-time signals, like TV signals.

To solve the problem of requiring the original work, a watermarking-based scheme can be a good candidate [6][7][9][10][11][12]. Such schemes can be used to assess im-

age/video quality by evaluating the similarity between the original watermark and the degraded watermark. The watermark is much smaller than the original work in size, which makes it easier to transmit and makes it possible for real-time quality evaluation. Good digital watermarking techniques are supposed to be able to embed watermarks invisibly with the least alterations to the cover works.

Of all the existed watermarking algorithms, the ones which serve the purpose of copyright protection and the content authentication become relatively mature. While using watermarking techniques to evaluate the quality of image/video is still a young research field.

The main idea of developing a watermarking based quality metric is that we can use the degradations of the watermark to evaluate the quality variations of the cover work [12][13][14]. We claim so, because the watermark is invisibly embedded throughout the active picture area to ensure the watermark embedding will not result in much quality degradation to the cover work. The watermark is inseparable with the cover work, which means the watermark will undergo the same transformations and distortions as the cover work. The watermark is embedded with suitable vulnerability, so that the degradation of the watermark can reflect the degradation of the cover work.

A typical watermarking based video/image quality evaluation system can be expressed in Fig. 1.6.

The watermark is embedded into the orthogonally transformed version of the original work. Then some distortions may be added during transmission. Next, the degraded watermark will be extracted in watermark extractor. And by comparing the degraded watermark with the original watermark, we can calculate the TDR (True Detection Rates) using [6][9]:

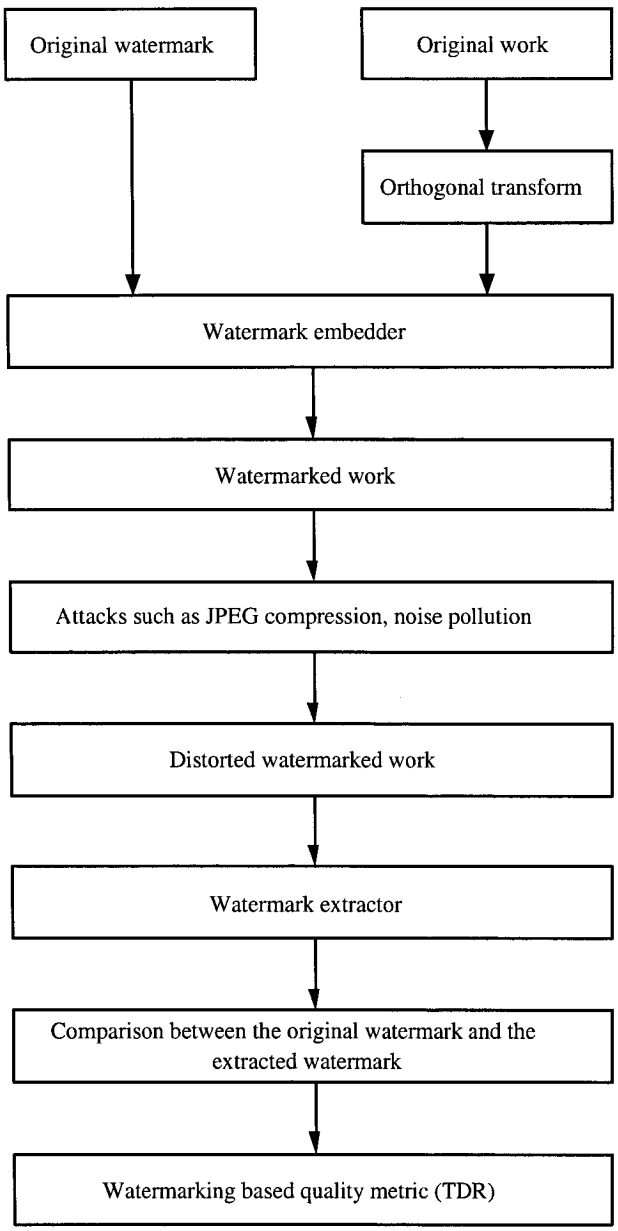

Figure 1.6: The watermarking-based quality measurement system

$$TDR = \frac{Number\ of\ correctly\ detected\ watermark\ bits}{Total\ number\ of\ watermark\ bits} \tag{1.12}$$

The orthogonal transform can be DWT, DCT, FFT, etc. And the possibility of successfully design such a quality metric can be proved using Fig. 1.8

Figure 1.7: The original watermark [23]

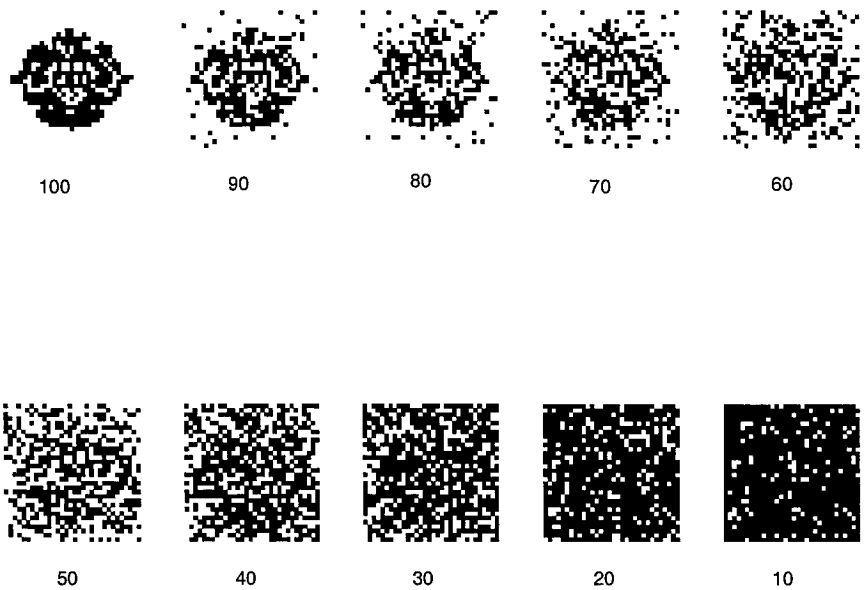

Figure 1.8: The watermark degradations

In Fig. 1.8, the numbers, from 100 to 10 with step -10, are the quality factors used in Matlab for JPEG compression. We can see, with the decreasing of the quality factor, the quality of the watermark drops, too. Thus, the quality degradation of the

watermark can roughly reflect the quality degradation of the compressed image. A more accurate watermarking-based quality evaluation scheme will be introduced in Chapter 3.

1.4 The contributions of the thesis

Based on the algorithm addressed in [26][27], we propose a semi-fragile watermarking scheme that can be used to evaluate image/video quality. The watermark is embedded into images/video frame with adjustable vulnerabilities. The vulnerability of watermark is different with respect to different frequency distributions of images/video frames. The contributions of this thesis include the idea of adjusting the watermark vulnerability according to different textured image/video frame, and the simple and feasible implementation of evaluating the image/video quality without the access to the original work.

We implement the algorithm and the experimental results show that the proposed scheme can be used to estimate image/video quality degradation under JPEG/MPEG-2 compression.

Publications generated from the research:

1. Sha Wang, Dong Zheng, Jiying Zhao, Wa James Tam, and Filippo Speranza, "A Digital Watermarking and Perceptual Model Based Video Quality Measurement," IEEE Instrumentation and Measurement Technology Conference, Ottawa, Ontario, Canada, 17-19 May, 2005.

2. Sha Wang, Dong Zheng, Jiying Zhao, Wa James Tam, and Filippo Speranza, "Video quality measurement using digital watermarking," IEEE Haptic,Audio

and Visual Environments and Their Applications,Ottawa, Ontario, Canada, pp. 183-188, 2-3 October, 2004.

3. Sha Wang, Jiying Zhao, Wa James Tam, and Filippo Speranza, "Image quality measurement by using digital watermarking based on discrete wavelet transform," The 22nd Biennial Symposium on Communications, Kingston, Ontario, Canada, pp. 210-212, 1-3 June, 2004.

1.5 Thesis structure

The thesis is organized as follows. In Chapter 2, we review several existing quality evaluation schemes. In Chapter 3, we propose our scheme. In Chapter 4, we address our experiment implementations in details. In Chapter 5, we illustrate and evaluate the proposed scheme. And in Chapter 6, we conclude the thesis and give some suggestions and ideas for future research work.

Chapter 2

Literature review

The problem of objective quality metrics, such as MSE and PSNR, is that they do not take any properties of human visual system into account. For still images/video, various factors could affect the subjective evaluation of quality including luminance masking, texture masking, etc. During the past decade, researchers have put lots of efforts on developing objective quality assessment metrics that can be used to estimate the subjective quality of the image/video. And more and more factors that may affect the visual effects are involved in the developments. All the existing quality evaluation metrics can be divided into two categories: the original-work-dependent algorithms, and the watermarking based algorithms.

The original-work-dependent algorithms [22][28] are those metrics evaluating quality with the access to the original work. They are still the most popular schemes used to measure the image/video quality. Most of the original-work-dependent schemes take some factors that may contribute to perceptual quality degradation of the cover work into account [22][24][37]. In these schemes, several masking thresholds are calculated and pooled into a single metric which is used to evaluate the quality. On the other

hand, some schemes evaluate the image/video quality directly using the statistical information, such as mean and variance, of the original work and the degraded work [28]. The schemes presented in [22] and [28] will be introduced in the following.

The watermarking based algorithms are to estimate the quality of the image/video using the watermark extracted from the degraded work. In this chapter, three frequently used watermarking schemes [10][29][30] will be presented as a brief summary of current researches in this field.

Makoto Miyahara et al proposed an original-work-dependent quality evaluation metric, picture quality score (PQS), in [22]. This score is achieved by processing the difference between the original work and the degraded work. Five possible errors and disturbances are considered, which may be caused by the objective distortion like JPEG compression or noise pollution, the human visual effects and the image coding errors. And under each possible factor, one masking threshold is calculated. The first one is a normalized noise-to-signal ratio in the spatial domain. The noise is the weighted difference between the original image and the distorted image in spatial domain. The second distortion factor describes the noise-to-signal ratio in frequency domain. The noise includes all the errors that exceed the perceptual threshold achieved by the contrast sensitivity function. The third distortion factor calculates the errors of the linear features in the image/video frames, because the HVS is more sensitive to linear features. This factor expresses all the horizontal and vertical block error discontinuities. The fourth distortion factor calculates the structural errors in the image. It is counted because of the strong spatial correlation in the image features and textures. The fifth distortion factor measures the errors in the vicinity of high contrast image transitions. Based on the properties of human visual system and the extensive engineering experiences on observing the image disturbances caused by image coding, the PQS is achieved

by linearly pooling the five calculated masking thresholds. The PQS ranges from 1 to 5 and is evaluated against the subjective mean opinion score (MOS). PQS is highly correlated with MOS with a correlation coefficient 0.92. And MSE correlates with MOS with 0.57. The proposed PQS is much more accurate to estimate the mean opinion score than the mean squared error.

Among the existing quality metrics, most of them are error-sensitivity based, including the one presented in [22]. That is to treat any quality degradation of image/video as a certain kind of error. On the other hand, according to the psycho-visual knowledge, the human eyes are more sensitive to structural errors than pixel errors. Aware of this point, some quality assessment schemes [28] are proposed based on evaluating the structural distortions of image/video.

In [28], an objective video quality evaluation metric is proposed based on estimating structural distortions of video sequence, frame by frame, using an 8 by 8 sliding window method. For one 8 by 8 block, mean and variance are calculated to classify the current block as smooth area or edge region or texture region. The structural distortions of each frame is estimated by averaging the distortions of the 8 by 8 blocks randomly selected from all the possible blocks of the frame. And the distortion of each block is calculated utilizing the statistical information, such as mean and variance, of the corresponding blocks in both the degraded work and the original work. The quality of the entire video can be evaluated by averaging the quality values of all the frames.

Although the schemes proposed in [22] and [28] possess different features, the common point of them is that all of their goals are reached by utilizing the spatial or frequency or statistical information of the original work.

For the convenience of evaluating image/video quality, some watermarking based objective quality metrics have been proposed in recent years, which have the big ad-

vantage of not requiring the access to the original image/video.

In such schemes, the watermark undergoes the same transformation and distortion as the original work. It is possible that the degradation of the watermark can reflect the degradation of the cover work. And the quality of the cover work can be estimated by evaluating the similarity between the degraded watermark and the original watermark.

The watermarking based quality evaluation theory is first proposed to estimate the quality of TV signals [12]. Directly, it can be employed in the schemes of blindly assessing quality of picture [10], video [29], audio [11] or used in other communication applications, like quality service of mobile communications [30]. Among the existing watermarking based quality evaluation schemes, two points are most critical: how to embed the watermark and where to embed it. For the first point, we have the choices to embed the watermark into the target work linearly [29], using the power spectrum method [30] or according to some user-defined rules [10][11][26]. And for the second point, we can embed the watermark according to the characteristics of the original work, such as frequency distribution, special picture areas we are interested in.

M.C. Faria et al [29] proposed a fragile watermarking based video quality assessment scheme utilizing the property of human visual system. The watermark location is determined by the amount of motion between the corresponding blocks of two consecutive frames. For the motion video sequence, it is stated that human viewers are more sensitive to the degradation/artifact of regions with large amount of motion. The regions with relatively small amount of motion are often regarded as the still background whose degradation in quality is often neglected by the human viewers. Based on this principle, the watermark is embedded into "moving areas" of the video. At the receiver, the watermark is extracted from the decoded video and a quality measure of the video is estimated by evaluating the degradation of the extracted mark. During embedding,

once the block with the amount of motion exceeding certain threshold is determined, the DCT is applied to this block. Then watermark is embedded by modifying the middle frequency DCT coefficients to minimize the quality degradation caused by the watermark embedding. Simulation results show that the results decrease monotonically with the PSNR of the degraded video which is compressed using MPEG-2 encoder with different bit rates setting. In this scheme, the watermark is linearly embedded into the selected DCT blocks. For the requirement of higher security, the watermark can be embedded into the cover work using the classic power spectrum method [30] of digital communications.

In [30], the fragile watermarking technique are applied to the classic wireless communication system in order to monitor the quality of service in time. The watermark is embedded in DCT domain for the convenience of using MPEG-2 compressed video. The same watermark is embedded into several selected frames. To make the perceptual distortion caused by the watermark embedding negligible, a unique spread matrix will be assigned to each selected video frame. Before embedding, the watermark is spread into a noise-like matrix using the uncorrelated pseudo-random spread sequence associated with the current video frame. When embedding, the narrow-band low-energy watermark is linearly embedded into the selected DCT coefficients of the frame. Its energy is spread over all the middle-high frequency components of the image. So, the watermark energy distributed in each selected frequency bin of the image is small enough to be negligible in order to meet the requirement of invisibility. At the receiver side, a matched filter is used to despread the watermark using the same PN sequence. The quality of the current video frame is evaluated using a normalized MSE calculated between the original watermark and the extracted watermark. And the overall quality of all the selected frames is estimated using the average of the calculated MSEs. The

watermarking technique is well used in the wireless communication system and the proposed idea is straightforward. It is effective to use the proposed scheme to blindly estimate the service quality.

Another widely used watermarking scheme for quality evaluation or authentication is to embed the watermark into the cover work by changing the frequency information of the cover work [10], [11] and [26]. These schemes are implemented in some orthogonal transform domain, such as DCT or DWT, and work according to some user-defined rules. The original work is first applied some orthogonal transform, such as DCT, DWT. The watermark is inserted into the cover work by slightly changing the selected middle-high frequency coefficients of the cover work according to the rules. The user-defined rules are to assign a binary bit 1 or 0 to each possible frequency coefficient. When embedding a watermark bit into a DCT/DWT coefficient, both of the watermark bit and the binary bit associated with the coefficient are checked. If they are equal, the current DCT/DWT coefficient will not be changed. If not, the DCT/DWT coefficient will be modified in order to make the binary bit associated with the modified coefficient equals to the watermark bit.

Using fragile/semi-fragile watermarking techniques to evaluate image/video quality is still a new research field. And the subjective quality evaluation is really a complicated topic to look into. Among the existing watermarking based quality evaluation metrics, the properties of human visual system are rarely considered. It will be much desirable to combine the relatively mature original-work-dependent quality evaluation techniques with the fragile/semi-fragile watermarking technique to make the watermarking based quality metrics effectively estimate the perceived quality of the image/video. The properties of human visual system, such as luminance masking, frequency sensitivity, contrast masking depicted in Section 1.3.2.2, and the psycho-visual theories that indi-

cate which parts of the image/video frames the human eye is more sensitive to should be used to guide the watermark embedding and optimize the selection of embedding locations.

Most of the existing quality evaluation schemes appear to measure the fidelity of the distorted work with respect to the original work, including all the papers we reviewed above. That is: the more similar the distorted work comparing with the original one, the higher the fidelity of the distorted work. A different concept of absolute image quality is introduced in [31]. By experiments, researchers find the sharpness and colorfulness can also heavily affect the perceptual quality of an image. "A reduction of sharpness or colorfulness from the original work to the distorted one corresponds to a decrease in perceived quality" [31]. The sharpness means high contrast and can be measured by evaluating the isotropic local contrast. The colorfulness can be determined by the average chroma and the spread of the distribution of the chroma values. The sharpness and colorfulness defined in the paper are designed to be able to work with any of the existing quality metric in order to give a comprehensive quality evaluation. With the involvement of the sharpness and colorfulness, the quality evaluation system is able to more accurately model the spatial-temporal contrast sensitivity functions of human visual system. Then the differences of the pattern sensitivity and contrast masking effects of both the original work and the distorted work will be calculated. The distortion measure can be achieved by pooling all the calculated differences together.

Although my current work is focused on the measurement of "fidelity", the absolute image quality surely is a research direction and can generate some inspiration about my current work.

Chapter 3

The proposed watermarking-based quality measurement scheme

The Discrete Wavelet Transform (DWT) is a good tool to decompose an image/video frame into different frequency components. In this thesis, the proposed scheme is based on DWT in order to adjust the vulnerability of the watermark. Before presenting the proposed scheme, we introduce the Discrete Wavelet Transform and its properties.

3.1 Discrete Wavelet Transform (DWT)

The DWT is defined as [42]:

$$W_{\varphi}(j_0, k) = \frac{1}{\sqrt{M}} \sum_{x} f(x) \varphi_{j_0,k}(x) \tag{3.1}$$

$$W_{\psi}(j, k) = \frac{1}{\sqrt{M}} \sum_{x} f(x) \psi_{j,k}(x) \tag{3.2}$$

where, $j \geq j_0$.

The Inverse DWT (IDWT) is defined as:

$$f(x) = \frac{1}{\sqrt{M}} \sum_k W_\varphi(j_0, k)\varphi_{j_0,k}(x) + \frac{1}{\sqrt{M}} \sum_{j=j_0} \sum_k W_\psi(j, k)\psi_{j,k}(x) \tag{3.3}$$

where $f(x)$ is the host signal, $\varphi_{j_0,k}(x)$ and $\psi_{j,k}(x)$ are two basis functions of the discrete variable. Normally we let $j_0 = 0$ and select M to be a power of 2 (i.e. $M = 2^J$) so that the summations in Equ. (3.1), Equ. (3.2) and Equ. (3.3) are performed over $x = 0, 1, 2, \cdots, J-1$, $j = 0, 1, 2, \cdots, J-1$ and $k = 0, 1, 2, \cdots, 2^j - 1$. The coefficients defined in Equ. (3.1) and Equ. (3.2) are respectively called approximation and detail coefficients.

$\varphi_{j,k}(x)$ is a member of the set of expansion functions achieved by translating and scaling a scaling function, $\varphi(x)$:

$$\varphi_{j,k}(x) = 2^{j/2}\varphi(2^j x - k) \tag{3.4}$$

$\psi_{j,k}(x)$ is a member of the set of expansion functions achieved by translating and scaling a wavelet function $\psi(x)$:

$$\psi_{j,k}(x) = 2^{j/2}\psi(2^j x - k) \tag{3.5}$$

The wavelet can be expressed as the filter bank operations. The two-scale equation is an important formula connecting the scaling function to itself at two different scales. The filter functions are defined by the two-scale equation implicitly.

$$\varphi(t) = \sum_k h_\varphi(k)\sqrt{2}\varphi(2t - k) \tag{3.6}$$

The orthonormal property for the scaling function is defined as:

$$\int_{-\infty}^{\infty} \varphi(t)\varphi(t-n)dt = \delta(n) \tag{3.7}$$

Shifting t by n in Equ. (3.6), we have

$$\varphi(t-n) = \sum_k h_\varphi(k)\sqrt{2}\varphi(2(t-n)-k) = \sum_k h_\varphi(k)\sqrt{2}\varphi(2t-(k+2n)) \tag{3.8}$$

Let $m = k + 2n$,

$$\varphi(t-n) = \sum_m h_\varphi(m-2n)\sqrt{2}\varphi(2t-m) = \sum_k h_\varphi(k-2n)\sqrt{2}\varphi(2t-k) \tag{3.9}$$

From Equ. (3.6), we can see that $h_\varphi(k)$ are the expansion coefficients of $\varphi(t)$ on the basis function $\sqrt{2}\varphi(2t-k)$. Similarly, in Equ. (3.9), $h_\varphi(k-2n)$ are the expansion coefficients of $\varphi(t-n)$ on the same basis function. Since we have the assumption in Equ. (3.7) and the basis functions are orthonormal, it is intuitive that:

$$\sum_k h_\varphi(k)h_\varphi(k-2n) = \delta(n) \tag{3.10}$$

So here we derive the Double shift orthogonality property of the filter function. If $n = 0$, we get $\sum_k h_\varphi^2(k) = \delta(0) = 1$. The same deviation is valid for the wavelet function, $\psi(t)$, and the filter $h_\psi(n)$:

$$\psi(t) = \sum_n h_\psi(n)\sqrt{2}\psi(2t-n) \tag{3.11}$$

To design the wavelet filters $h(n)$ including $h_\varphi(n)$ and $h_\psi(n)$, the following properties of the filters must be observed:

1. Normalization: $\sum_k h^2(k) = 1$.
2. Double shift orthogonality: $\sum_k h(k)h(k-2n) = 0, n \neq 0$.
3. Low pass filter $h_\varphi(n)$: $\sum_k (-1)^k h_\varphi(k) = 0$.
4. High pass filter $h_\psi(n)$: $h_\psi(k) = (-1)^k h_\varphi(N-k)$.

For example, the filter functions of the length 2 Haar wavelet are $h_\varphi = [1/\sqrt{2}, 1/\sqrt{2}]$, and $h_\psi = [1/\sqrt{2}, -1/\sqrt{2}]$.

The *db*-2 length 4 wavelet filters have the following filter bank ($\alpha = \frac{\pi}{3}$):

$$h_\varphi(0) = \frac{1 - cos\alpha + sin\alpha}{2\sqrt{2}} \tag{3.12}$$

$$h_\varphi(1) = \frac{1 + cos\alpha + sin\alpha}{2\sqrt{2}} \tag{3.13}$$

$$h_\varphi(2) = \frac{1 + cos\alpha - sin\alpha}{2\sqrt{2}} \tag{3.14}$$

$$h_\varphi(3) = \frac{1 - cos\alpha - sin\alpha}{2\sqrt{2}} \tag{3.15}$$

And $h_\psi(0) = h_\varphi(3), h_\psi(1) = -h_\varphi(2), h_\psi(2) = h_\varphi(1), h_\psi(3) = -h_\varphi(0)$, which are obtained by solving the above properties of wavelet filters.

Since The DWT can be formulated as a filtering operation with two related FIR filters, low-pass filter h_φ and high-pass filter h_ψ. Both $W_\varphi(j,k)$ and $W_\psi(j,k)$, the scale j

approximation and the detail coefficients, can be computed by convolving $W_\varphi(j+1,k)$. The scale $j+1$ approximation coefficients, with the time-reversed scaling and wavelet vectors, $h_\varphi(-n)$ and $h_\psi(-n)$, and

$$W_\psi(j,k) = h_\psi(-n) * W_\varphi(j+1,n)|_{n=2k,k\geq 0} \tag{3.16}$$

$$W_\varphi(j,k) = h_\varphi(-n) * W_\varphi(j+1,n)|_{n=2k,k\geq 0} \tag{3.17}$$

Sub-sampling the results by 2, expressed in Equ. (3.16) and Equ. (3.17) and illustrated in Fig. 3.1.

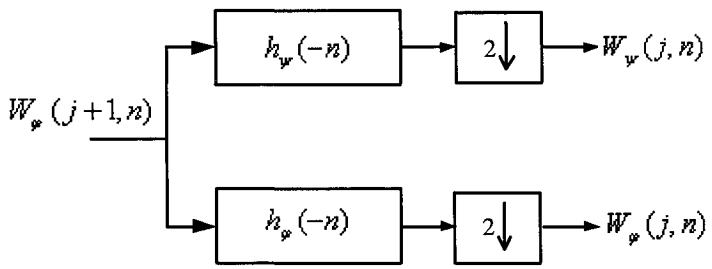

Figure 3.1: A DWT analysis bank

The filter bank in Fig. 3.1 can be iterated to implement multi-solution analysis. The IDWT can be implemented by up-sampling and synthesis filtering. The one-dimensional DWT and IDWT can be extended to two-dimensional.

Wavelet algorithms are recursive and the smoothed data d_i becomes the input for the next step of the wavelet transform. A widely used example is the Haar wavelet filters whose low pass filter is $H_\varphi(\omega) = \frac{1}{2} + \frac{1}{2}e^{-j\omega}$ and high pass filter is $H_\psi(\omega) = \frac{1}{2} - \frac{1}{2}e^{-j\omega}$.

To ensure the IDWT and DWT relationship, the following orthogonality condition is necessary:

$$|H_\varphi(\omega)|^2 + |H_\psi(\omega)|^2 = 1 \tag{3.18}$$

As stated in [43]: "Orthonormal transforms are of interest because they can be used to re-express a time series in such a way that we can easily reconstruct the series from its transform." In other words, we can reconstruct the signal inversely from its decomposed wavelet coefficients without loss of information.

We can easily extent the wavelet to the two dimensional image processing as shown in:

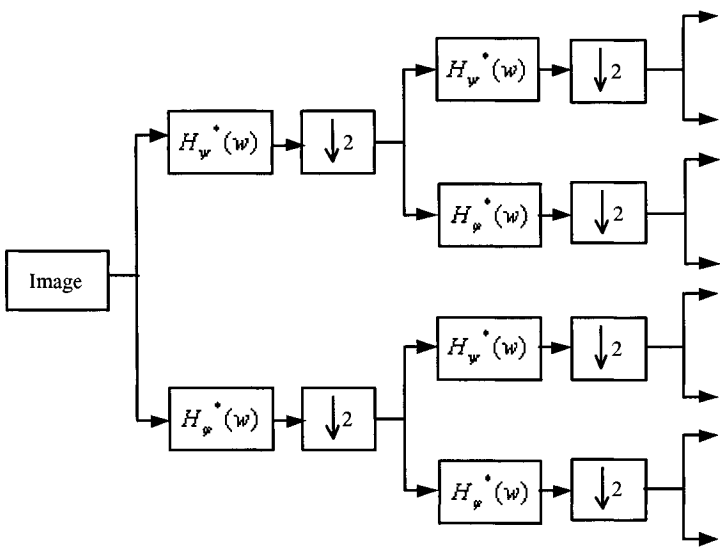

Figure 3.2: DWT down-sampling

There are lots of other wavelet filters such as the Daubechies wavelet transform, which have their own wavelet and scaling functions. The pyramid structure of the decomposed image is as following:

In Fig. 3.3, LL3 is the approximation coefficient block. And the other 9 blocks are the detail coefficient blocks. In this thesis, we denote block HL1, LH1 and HH1 as the

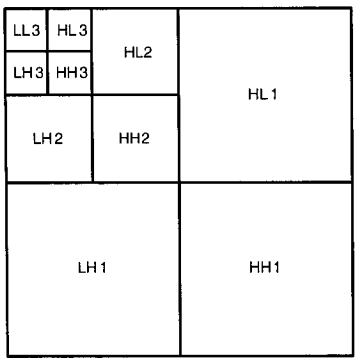

Figure 3.3: DWT decomposed blocks

blocks in the first DWT level; block HL2, LH2 and HH2 as the blocks in the second DWT level; block HL3, LH3 and HH3 as the blocks in the third DWT level. And as the approximation coefficient block, LL3 is denoted as the block in the 0 DWT level to distinguish it with the other 9 detail coefficient blocks.

3.2 Characteristics of the DWT decomposed blocks under compression

For the DCT based JPEG and MPEG compression, the frequency distribution of the image/video frame has a great effect on how its quality degrades (PSNR) when compressed with different quality factors (JPEG) or compression rates (MPEG). If we want to design a watermarking-based quality measurement scheme which is faithful to the PSNR, the frequency distribution of the image/video frame has to be taken into account. Discrete wavelet transform is a good tool to decompose the image into different frequency components [33][40]. If we apply 3-level DWT to the original images Lena and Baboon, we can get the wavelet decomposed blocks and put them in the pyramid

(a) The original Lena

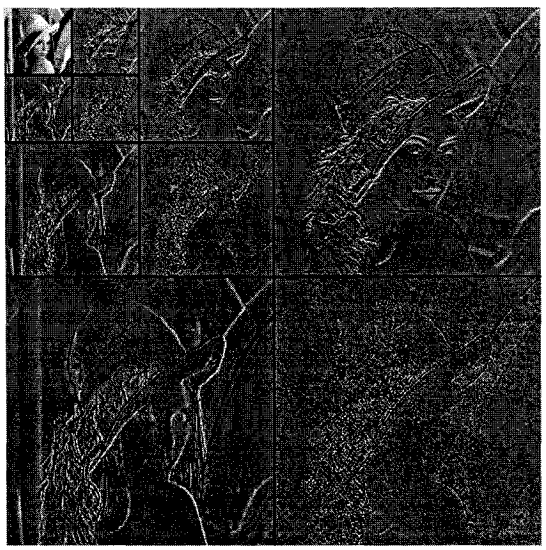

(b) 3-level wavelet decomposed Lena

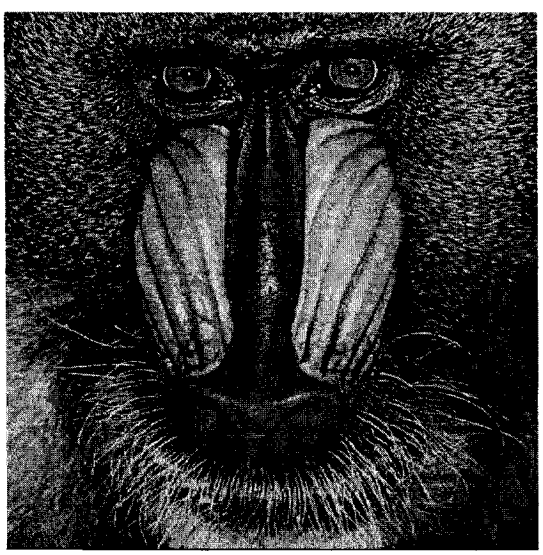

(c) The original Baboon

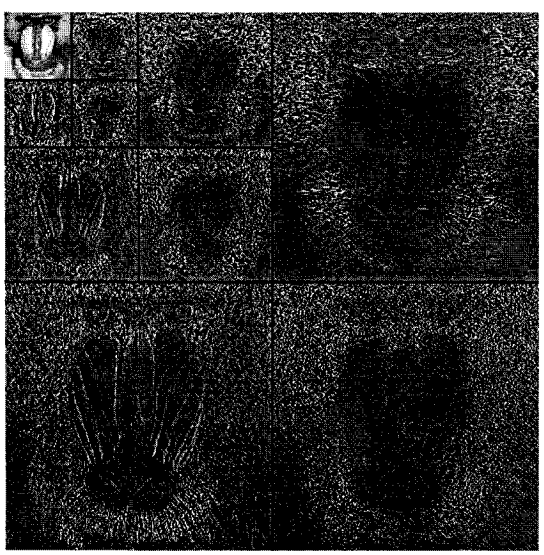

(d) 3-level wavelet decomposed Baboon

Figure 3.4: The original Lena and Baboon with their wavelet decomposed images

structure as shown in Fig. 3.4 (b) and (d).

By observing the images Lena and Baboon, we can have a general impression on their image characteristics. The image Lena has a girl head in the center and some bland background around. It can be assumed that the image Lena has a wide variety of frequency components. The image Baboon has a large monkey head with lots of hair and beard. So it can be assumed that the most dominant frequency components in image Baboon are high frequency components. These assumptions can be illustrated in Fig. 3.4, where Baboon has much more components in the detail coefficient blocks than Lena.

Recall Equ. (3.16) and Equ. (3.17), the detail coefficient blocks in the 2^{nd} or 3^{rd} DWT level are obtained by decomposing the approximation coefficient block in their previous DWT level. Thus, the detail coefficients in the first-level blocks are relatively higher frequency ones comparing with those in the second-level blocks. And the detail coefficients in the second level are higher frequency ones comparing with those in the third level. Based on this analysis, under the same distortion, the blocks in different levels will behave differently.

Under JPEG compression, the performances of the decomposed blocks of Lena and Baboon can be illustrated in Fig. 3.5 and Fig. 3.6. And the quality degradation of the whole image and the blocks' contributions to the quality loss of the image can be evaluated using PSNR.

In these figures, the quality factors used in Matlab indicate the compression ratios. The higher the quality factor, the lower the compression ratio. The solid curves are the quality degradations of image Lena and Baboon with quality factors varying from 10 to 100 with step 10. The performance of the block in Level 0 indicates the contribution of the approximation block to the quality degradation of the image. Performance of

the blocks in Level 1 indicates the average behavior of the 3 detail coefficient blocks in Level 1 under JPEG compression. So do the other curves in the figures.

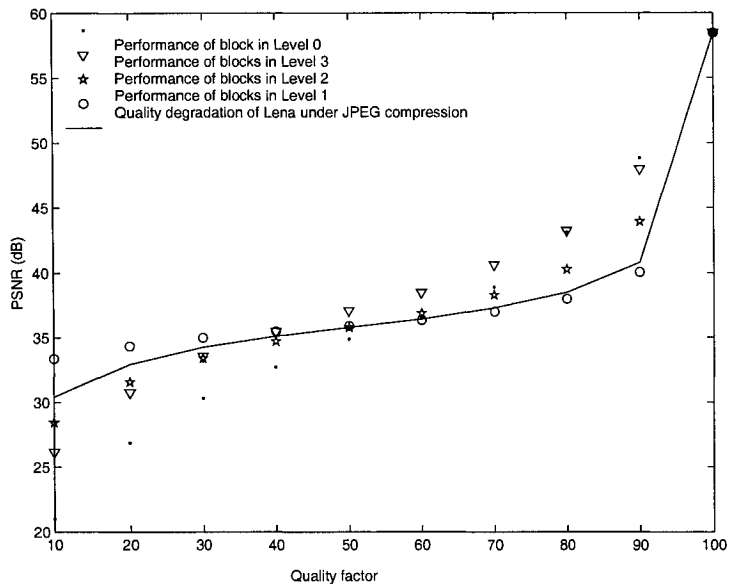

Figure 3.5: The contributions of the decomposed blocks in each level to Lena's quality degradation

Fig. 3.5 shows the PSNR change of image Lena and the PSNR changes of the blocks in different DWT level. When the quality factor is large, the JPEG compression affects the high frequency mostly. With the quality factor becoming smaller and smaller, the middle frequency and low frequency components are starting to be affected by the JPEG compression.

Fig. 3.6 shows the PSNR change of the Baboon image. It can be seen that the PSNR curve of the whole image fits well with the average PSNR change of the blocks in DWT level 1, since the wavelet Level 1 consists of rich high frequency components. This result shows that the assumption that the DWT can decompose an image into different frequency components is reasonable.

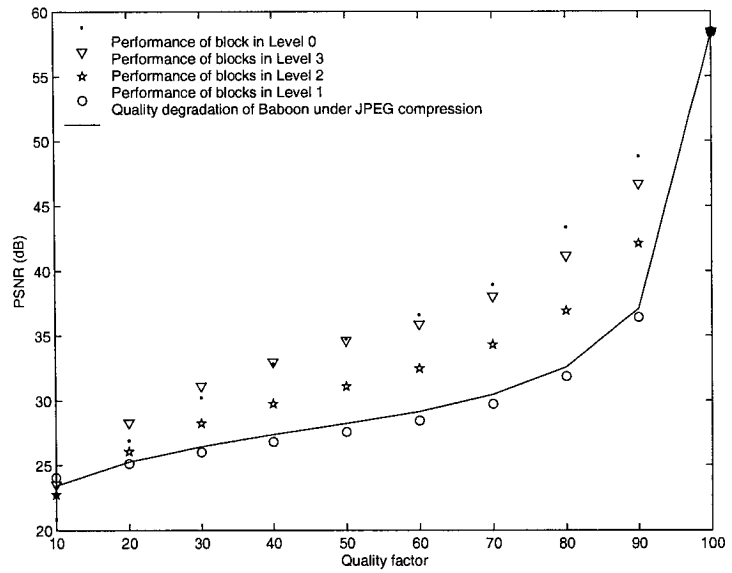

Figure 3.6: The contributions of the decomposed blocks in each level to Baboon's quality degradation

Different frequency blocks have different sensitivities to compression. Therefore, if we embed different watermark bits into different frequency blocks with different embedding strength, we will have watermarks with different vulnerabilities. For example, we can embed fewer watermark bits into the relatively low frequency blocks with smaller embedding strength to keep the fidelity. And we can embed fewer watermark bits into the relatively high frequency blocks with bigger embedding strength to reduce the watermark sensitivity. We also can embed more watermark bits with suitable embedding strength to control the balance between the fidelity and robustness. By doing so, we can control the watermark degradation.

3.3 Quantization

In MPEG-2 compression, quantization is used to reduce information redundancy. The quantization technique can be modelled as [24]:

$$x_q = \left\lfloor \frac{x}{q} + 0.5 \right\rfloor \tag{3.19}$$

where, x is the original coefficient, q is the quantization step, and x_q is the quantized coefficient achieved by rounding the $\frac{x}{q}$ to its nearest integer. For image/video, the larger the quantization steps, the lower the image/video quality.

The inverse quantization can be presented as:

$$x' = x_q \times q \tag{3.20}$$

where x' is the regenerated integer by inverse quantization. And x' is normally not equal to x. Therefore the quantization process is lossy.

Most common lossy compression algorithms first transform the original signals into a different domain such as Discrete Cosine Transform (DCT), Discrete Fourier Transform (DFT) or Discrete Wavelet Transform (DWT) domain. Then, each of the resulting coefficients is independently quantized.

In JPEG/MPEG-2 compression, images/video frames are compressed by reducing the relatively high frequency components with respect to the compression ratio [32]. And this reduction is realized by quantizing the DCT coefficients. Because human viewers are more sensitive to the low frequency components, smaller quantization steps are assigned to the lower frequency coefficients [38]. Table 3.1 is a classic 8 by 8 quantization table used for the Intra frames in MPEG-2.

Table 3.1: Quantization table for Intra frames in MPEG-2 compression

8	16	19	22	26	27	29	34
16	16	22	24	27	29	34	37
19	22	26	27	29	34	34	38
22	22	26	27	29	34	37	40
22	26	27	29	32	35	40	48
26	27	29	32	35	40	48	58
26	27	29	34	38	46	56	69
27	29	35	38	46	56	69	83

The upper left value, 8, in Table 3.1 is the quantization step for the DC component in each 8 by 8 DCT block. The bottom right value, 83, is the quantization step for the highest frequency component.

Quantization is being used by many robust or semi-fragile watermarking algorithms. A robust watermarking algorithm need survive the quantization process, while an ideal semi-fragile watermarking algorithm need provide fragility that is proportional to the quantization step size q.

Quantization has the following property [24]. Let $x \diamond q$ be the result of quantizing x to an integral multiple of the quantization step size, q:

$$x \diamond q = q \left\lfloor \frac{x}{q} + 0.5 \right\rfloor \tag{3.21}$$

If a is a read-valued scalar quantity, and q_1 and q_2 are quantization step sizes, with $q_2 \leq q_1$, then

$$((a \diamond q_1) \diamond q_2) \diamond q_1) = a \diamond q_1 \tag{3.22}$$

The feature represented by Equ. (3.22) guarantees that if a quantization-based

watermark is embedded by using quantization step size q_1, it will be detectable even after the host signal is re-compressed by using quantization step size q_2 ($q_2 \leq q_1$).

3.4 The proposed watermarking-based video quality measurement scheme

A new watermarking-based objective video quality measurement method is proposed in this section. The schemes are applied in the procedures of MPEG-2 compression and decompression. And the watermark embedding and extraction are implemented in DWT domain. Fig. 3.7 is the proposed video quality measurement system.

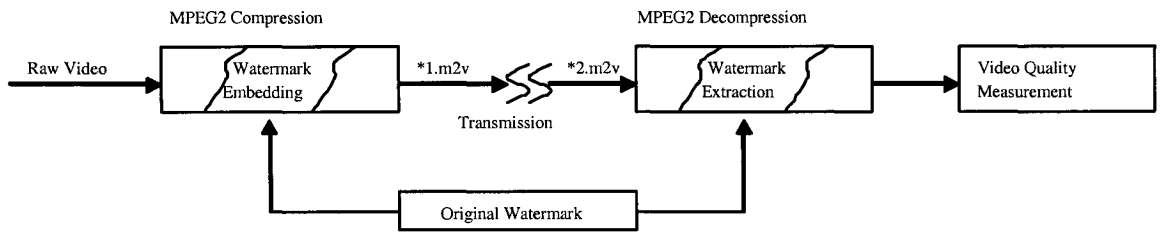

Figure 3.7: Watermarking-based video quality measurement system

Among the I, P, B frames in an MPEG-2 video, the I frame carries the main information of the current group of pictures. P and B frames bring the predictive errors. Through experiments, we find both P and B frames are very sensitive to attacks, even small changes. Fully noticing the importance and characteristics of I frames, we choose to embed watermark in the luminance components of the I frames of the source video.

Video quality is estimated by evaluating the watermark degradation. Meanwhile, at the receiver side and without the original work, the quality should be estimated in terms of some widely used quality metrics, such as PSNR, or wPSNR, or Watson

JND. Therefore, it will be easier to evaluate the accuracy of the quality estimation. As analyzed in Section 3.2, the watermark degradation can be controlled by embedding different watermark bits into different frequency blocks with different embedding strength, according to the approximate frequency distribution of different images. Therefore, the two tasks we need to accomplish are: to find a balance between robustness and fidelity, and to improve the accuracy of the quality estimation.

In this chapter, we propose a watermarking-based video quality measurement scheme. The video quality can be measured by evaluating the watermark degradation. Our method indicates the possibility to control the watermark degradation and the possibility to improve the accuracy of the evaluation result. Meanwhile, this idea eliminates the need for the original work when we estimate video quality at the receiver side.

The details of the watermark embedding including the automatic adjustment of the watermark vulnerability, and the details of the watermark extraction and quality measurement will be discussed in Chapter 4

Chapter 4

Implementation

4.1 Automatic control theory used in the proposed scheme

Automatic control is to make the measured output match the desired output as much as possible [44][45][46]. Fig. 4.1 is a typical unit-step response of a control system and can give us a rough idea about how the control system works [46].

In Fig. 4.1, the straight line is the reference input which is also named as desired output. The curve is the measured output.

The maximum overshoot is defined as the difference between the maximum value of the measured output and the desired output.

Rise time is the time required for the step response to rise from 10% to 90% of the final output.

Steady-state error is the discrepancy between the output and the desired output when steady-state is reached or when t goes to infinity.

Setting time is the time required for the step response to decrease and stay within

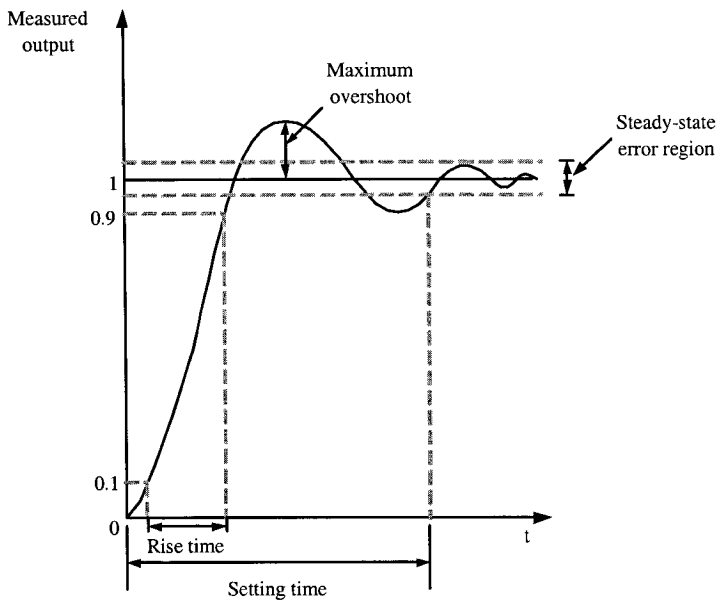

Figure 4.1: A typical unit-step response of a control system illustrating the time-domain specifications

the specific range of steady-state error which defines the acceptable experimental errors.

When automatically controlling a process, the shorter the setting time, the better. So does the rise time. And the smaller the maximum overshoot, the better. So does the steady-state error.

When designing an automatic control system, the designers always give some empirical information to the system to make the measured output goes to the desired output as closer as possible. And by this way, the rise time is shortened. This preliminary step is always called as rough adjustment. After the rough adjustment, the error between the measured output and the desired output will be fed-back to the system and guide it to make it stable. This step is implemented automatically and called as fine adjustment.

Recall the feedforward control system and feedback control system, which are re-

spectively shown in Fig. 4.2 and Fig. 4.3.

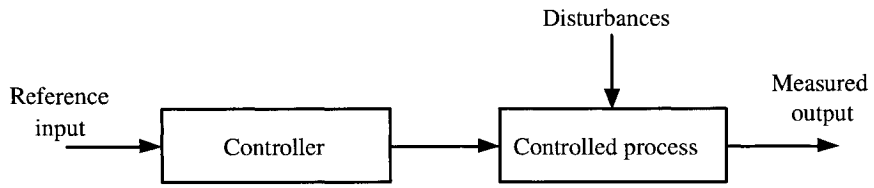

Figure 4.2: The feedforward control system

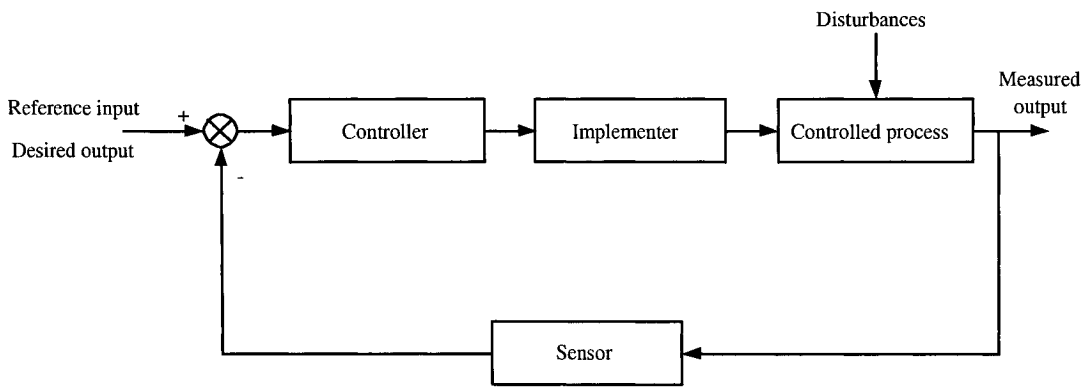

Figure 4.3: The feedback control system

The feedforward control systems are also called as open-loop system, which works according to some prescribed standards. Because no signals are used to control the system, the designers always provide the system with some important empirical information. The advantages of such systems are that they can be easily realized, and can spare much time and cost.

Feedback control systems are also called as close-loop system. The aim of feedback control is to eliminate or reduce the errors between the desired output and the measured output. Such systems have good control effects, but sometimes they are time-consuming.

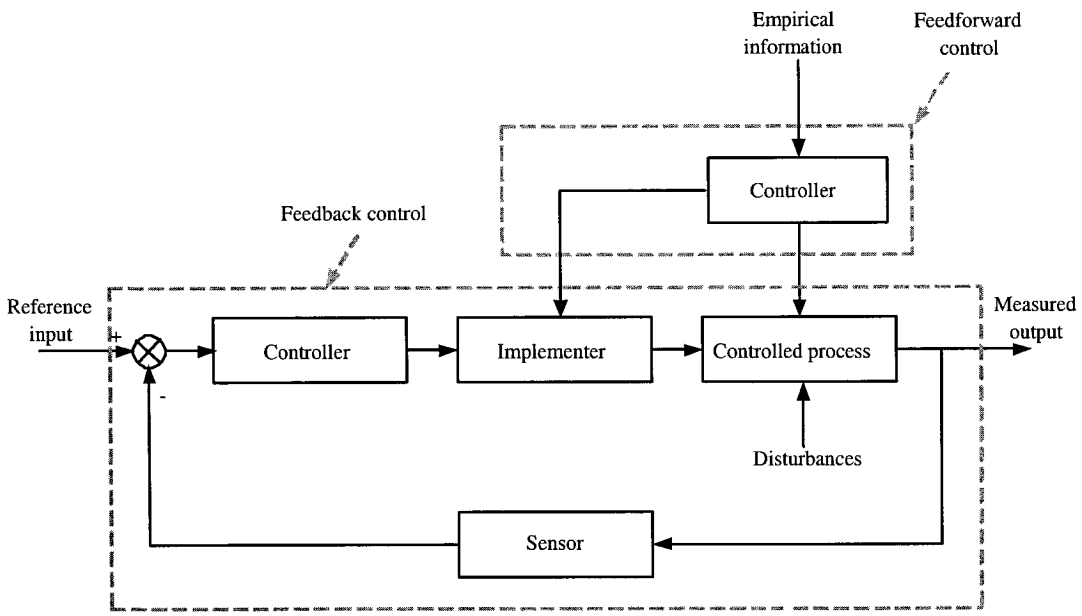

Figure 4.4: The automatic control system designed

In this thesis, to combine the advantages of both the feedforward control system and feedback control system, an automatic control system is designed as shown in Fig. 4.4. The feedforward control is used to coarsely adjust the vulnerability of the watermark according to the approximate frequency distribution of the cover image. And feedback control is used to finely adjust the vulnerability of the watermark according to the accuracy requirement of the experiment.

4.2 Watermark embedding scheme

The "image" shown in this section indicates the luminance component of the I frame where the watermark is embedded. A feedforward control and a feedback control are added to the watermark embedding process.

Fig. 4.5 shows the proposed watermark embedding scheme. The steps of embedding watermark are as follows:

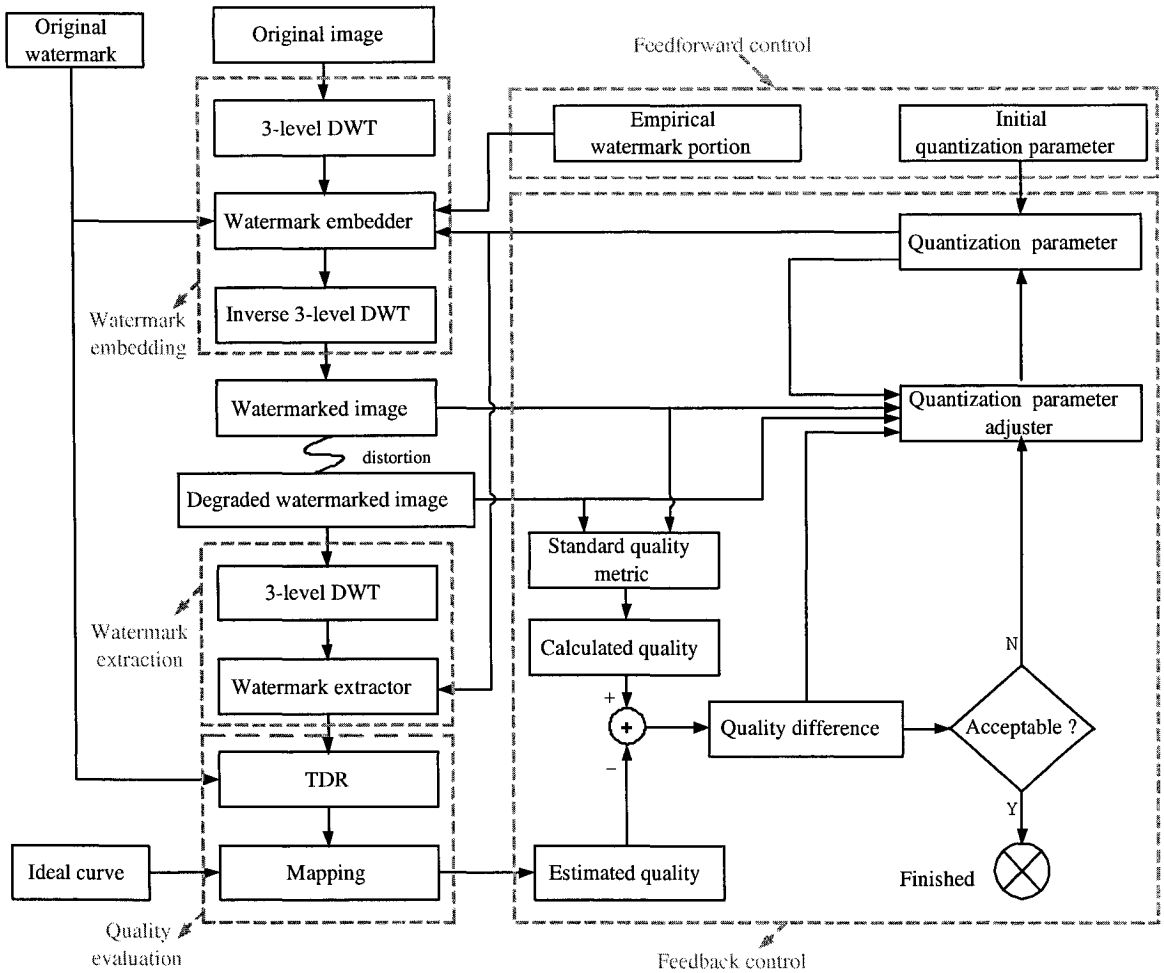

Figure 4.5: The proposed watermark embedding scheme

1. Embed the watermark into the original image.

   (a) Apply 3-level DWT to the original image and we get 10 DWT decomposed blocks as numbered in Fig. 4.6.

(b) Embed the watermark into the selected DWT coefficients using the feedforward control.

(c) Apply inverse 3-level DWT to the watermarked DWT coefficients.

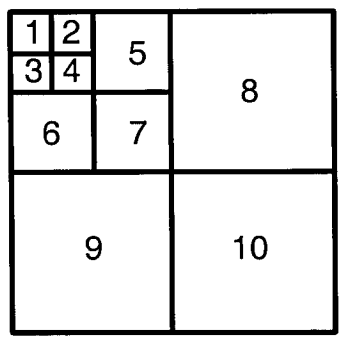

Figure 4.6: Wavelet decomposition

2. Obtain the watermarked image.

3. Attack the watermarked image to simulate some possible distortions in the transmission procedure.

4. Obtain the degraded watermarked image.

5. Extract the degraded watermark from the degraded watermarked image.

   (a) Apply 3-level DWT to the degraded watermarked image.

   (b) Extract the degraded watermark.

6. Pre-evaluate the image quality in order to improve the accuracy of quality estimation.

   (a) Compute the True Detection Rate between the original watermark and the degraded watermark.

(b) Map the TDR to estimated quality according to the pre-calculated ideal mapping curve.

7. Improve of the accuracy using the feedback control.

   (a) The difference is calculated between the calculated quality and the estimated quality which is obtained from Step 6.

   (b) Check whether the difference is acceptable. If it is acceptable, goto Step 8. If it is unacceptable, adjust the quantization parameters according to the difference and repeat the above steps with the adjusted quantization parameters.

8. Output the watermarked image and the adjusted quantization parameters.

In the watermark embedding procedure, a quantization-based method is used to embed watermark into the selected DWT coefficients.

4.2.1 Quantization method used for watermark embedding

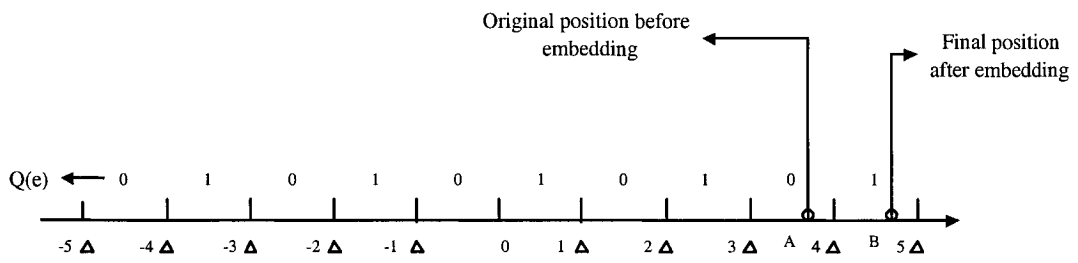

Figure 4.7: The quantization of DWT coefficients

Fig. 4.7 shows us the details of the quantization method used for watermark embedding.

Before the watermark embedding, we first order the DWT coefficients from the biggest to the smallest in each DWT block. Then every DWT coefficient will be quantized using Equ. (4.1). By doing so, each coefficient will be assigned a binary 1 or 0. And we call this binary sequence as $Q(e)$.

$$Q(e) = \begin{cases} 1 & \left\lfloor \frac{DWT\ coefficient}{Quantization\ parameter} \right\rfloor \ is\ even \\ 0 & \left\lfloor \frac{DWT\ coefficient}{Quantization\ parameter} \right\rfloor \ is\ odd \end{cases} \tag{4.1}$$

When we embed a watermark bit into a target DWT coefficient, we first check whether the binary bit associated with the target DWT coefficient equals to the watermark bit. If they are equal, we do not make any changes. If they are not equal, we modify the target DWT coefficient by adding a quantization parameter to it in order to make the binary bit associated with the modified coefficient equal to the watermark bit.

An example of watermark embedding is shown in Fig. 4.7. We want to embed a watermark bit 1 into coefficient A whose binary bit is 0. And the watermark bit is not equal to the binary bit of the coefficient. Then we add a quantization parameter to A to change A to B. And the binary bit of B is 1. The watermark bit equals to the binary bit of the modified coefficient. Therefore, this watermark bit is embedded into the target coefficient.

Each watermark bit is embedded into the 50 biggest DWT coefficients of the remained coefficients to add some redundancy for the detection of the watermark bit. That is, the first watermark bit is embedded into the first 50 biggest DWT coefficients of the block; and the second watermark is embedded into the next 50 biggest DWT coefficients of the block and so on.

4.2.2 Feedforward control

The feedforward control is a coarse adjustment and is used to set similar initial vulnerabilities for watermarks embedded in images. It consists of two components: the empirical watermark bit portion and the initial quantization parameters.

The watermark bit portion indicates how many watermark bits are embedded into one DWT decomposed block. It is a percentage of the watermark bits embedded in one block over the total watermark bits. For example, we can decide the watermark bit portions according to the percentage of the area of the wavelet decomposed block, shown in Fig. 4.6, out of the total size of the image. In this case, we divide the watermark into 10 sub-blocks using the same scale as shown in Fig. 4.6. Then each watermark sub-block will be embedded into the corresponding DWT decomposed block of the image. Obviously, the 1^{st} wavelet block accounts for the 1/64 of the total size of the image, so the watermark bit portion for this block is 1/64. Similarly, the watermark portions for the 2^{nd}, 3^{rd} and 4^{th} wavelet decomposed blocks can also be calculated as 1/64. The watermark bit portions for the 5^{th}, 6^{th}, 7^{th} watermark block can be calculated as 1/16. The watermark bit portions for the 8^{th}, 9^{th}, 10^{th} wavelet block can be calculated as 1/4. Thus, we have 10 watermark bit portions, [1/64,1/64,1/64,1/64,1/16,1/16,1/16, 1/4, 1/4, 1/4], for the 10 wavelet decomposed blocks of the image. For convenience, we only need to record 3 watermark bit portions, one for the smallest blocks in the same size (1, 2, 3, and 4), the second for the medium blocks (5, 6, and 7) and the third one for the largest blocks (8, 9, and 10). And in this case the watermark bit portion matrix can be denoted as [1/64,1/16,1/4] which can be also expressed as [0.015625, 0.0625, 0.25].

Based on the analysis in Section 3.2, the empirical watermark portions, [0.0479, 0.25, 0.0195], tested in [7] are used in the thesis experiments.

The quantization parameters control the embedding strength of the watermark. 10 quantization parameters are assigned to the 10 DWT decomposed blocks. The initial quantization parameters are set as [80 80 80 80 80 80 80 80 80 80]. They are tested using the empirical watermark portions with the quantization parameters varying from 10 to 200 with a step of 5.

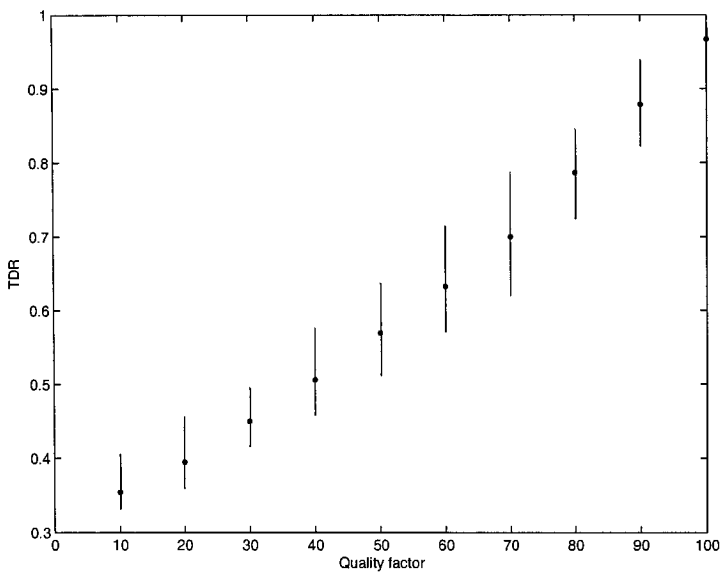

Figure 4.8: The TDR variations calculated using only feedforward control

With the feedforward control, the PSNR values of the undistorted watermarked images are better than 40 dB. And the calculated TDRs vary in limited ranges as shown in Fig. 4.8. Fig. 4.8 shows the test results on 10 different textured images with JPEG quality factor from 100 to 10 with a step of 10. The dots are the mean TDR. And the bars indicate the variation ranges of the TDR values.

Therefore, we can set initial states for watermark embedded in different images with feedforward control. On the other hand, Fig. 4.9 shows the results tested on Lena and Baboon. It is shown in the figure that we can not use the TDR to estimate the PSNR

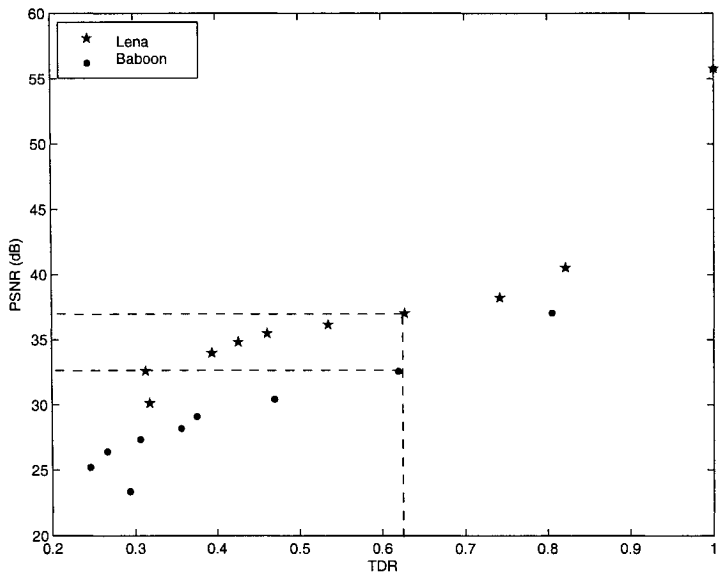

Figure 4.9: PSNR vs. TDR calculated with only feedforward control

since the PSNRs of Lena and Baboon are quite different when the TDRs of Lena and Baboon are the same. So we need to use the fine adjustment to make it possible to use the TDR to estimate the PSNR. Then we introduce the feedback control to improve the accuracy of the experiment.

4.2.3 Feedback control

The feedback control is used to improve the accuracy of the experimental results. It is to finely adjust the vulnerability of the watermark using the feedback information by adjusting the quantization parameters as shown in Fig. 4.5. The feedback control consists of two components: the quality difference calculation and the quantization parameter adjustment.

The quality difference calculation is to calculate the difference between the quality evaluated by the proposed method and the quality calculated by the standard quality

metrics (PSNR, wPSNR, or Watson JND). If the quality difference is larger than some threshold (i.e. 4.5 dB or 4.5 JND for the summation of the quality differences under 9 quality factors from 100 to 20 with a step of -10), the quantization parameter adjuster will continue to adjust the quantization parameters. If the quality difference is still beyond the threshold after 15 iterations, the watermarked image and the quantization parameters with the smallest quality difference will be output.

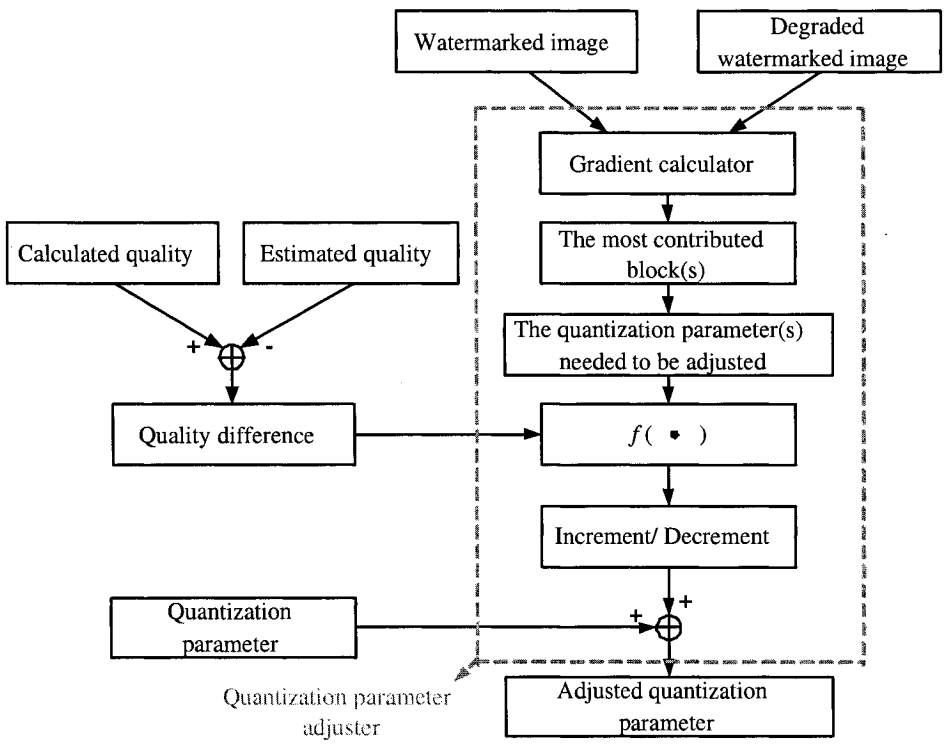

Figure 4.10: The quantization parameter adjustment

The quantization parameter adjuster works by checking the DWT decomposed blocks' contributions to the current quality loss. As shown in Fig. 4.10, the quantization parameters are automatically adjusted according to the quality difference calculated between the calculated quality and the estimated quality. The estimated quality

is obtained by mapping TDR according to the ideal mapping curve. The function $f(\bullet)$ is used to estimate the increment or decrement for the quantization parameters that need to be adjusted. The quantization parameter of the block that contributes the most to the current quality loss will be adjusted according to the quality difference. Therefore, before adjustment, we need to find which quantization parameter needs to be adjusted and the increment or decrement for it.

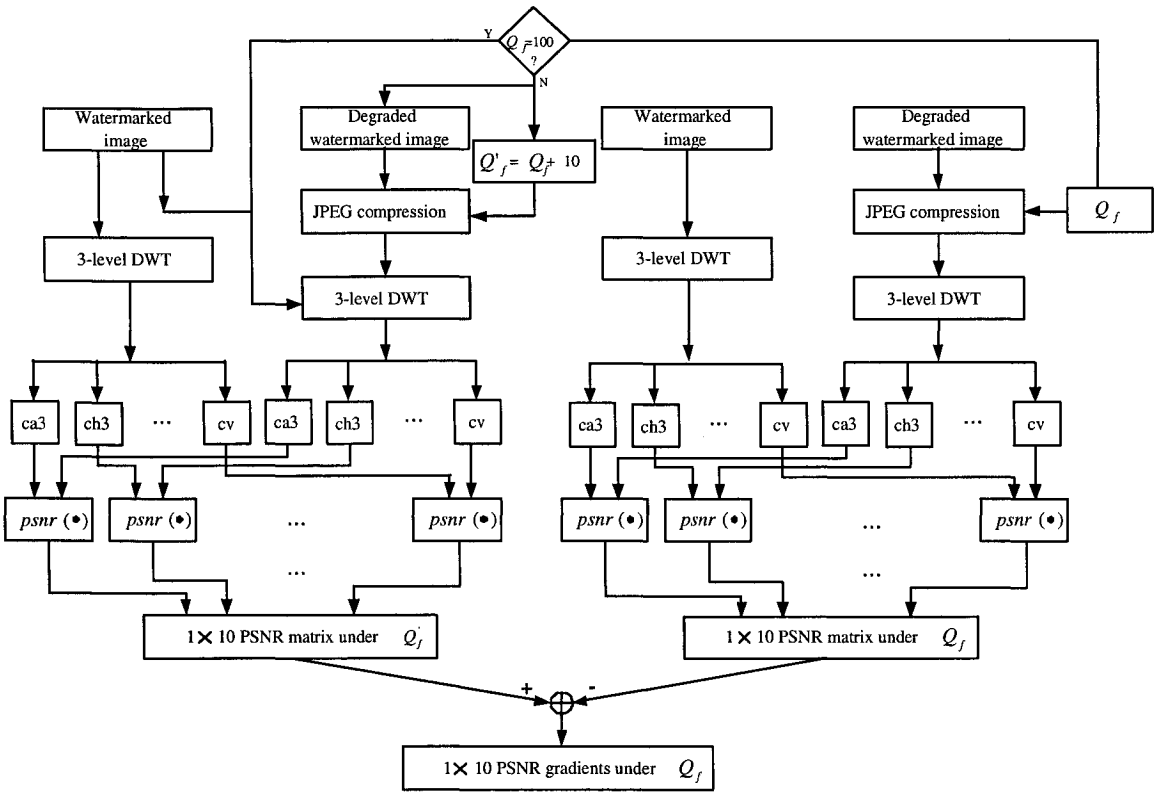

Figure 4.11: The gradient calculator

The gradient calculator is used to estimate the sensitivities of the DWT decomposed blocks to compression. The larger the calculated gradient, the more sensitive the block to compression. The block with the largest gradient is the one whose quantization parameter has the largest effect on changing the vulnerability of the watermark. Fig.

4.11 shows some details of the gradient calculator used for estimating image quality in terms of PSNR. It can also be used to find the most contributing blocks for estimating wPSNR or Waston JND by changing the $psnr(\bullet)$ in Fig. 4.11 to $wpsnr(\bullet)$ or $jnd(\bullet)$.

Therefore, the summarized steps of feedback control using the gradient calculator shown in Fig. 4.11 are:

1. Calculate quality difference between the calculated quality and the estimated quality under all Q_F.

$$\Delta Quality(Q_F) = Calculated\_Quality(Q_F) - Estimated\_Quality(Q_F) \quad (4.2)$$

where, Q_F is the JPEG quality factor varying from 100 to 20 with a step of -10.

2. Find the block that contributes the most to the quality loss using the gradient calculator shown in Fig. 4.11.

   (a) Apply 3-level DWT to the undistorted watermarked image $I^w(k)$, we get the 10 wavelet decomposed blocks $I_i^w(K)$.

$$I^w(k) \longrightarrow I_i^w(K), \qquad (i = 1, \cdots, 10). \quad (4.3)$$

   (b) Apply 3-level DWT to the compressed watermarked image $I^{wD}(k, Q_F)$ to obtain the corresponding wavelet decomposed blocks $I_i^{wD}(K, Q_F)$. The compressed watermarked image is got by compressing the watermarked image with a quality factor Q_F.

$$I^{wD}(k, Q_F) \longrightarrow I_i^{wD}(K, Q_F), \qquad (i = 1, \cdots, 10). \quad (4.4)$$

(c) Respectively calculate the PSNRs between the corresponding DWT decomposed blocks of the watermarked image and the compressed watermarked image using the Equ. (1.4). For example, we calculate the PSNR between the first block of the undistorted watermarked image, $I_1^w(K)$, and the first block of the compressed watermarked image, $I_1^{wD}(K, Q_F)$. Applying this procedure to all the corresponding blocks:

$$PSNR(i, Q_F) = psnr(I_i^w(K), I_i^{wD}(K, Q_F)) \qquad (i = 1, 2, \cdots, 10) \quad (4.5)$$

where, $PSNR$ is the value calculated using the function $psnr$.

(d) Calculate the PSNR gradients $G(i, Q_F)$ under Q_F for all the 10 blocks using Equ. (4.6).

$$G(i, Q_F) = \begin{cases} PSNR(i, Q_F + 10) - PSNR(i, Q_F) & if\ Q_F < 100 \\ \\ PSNR(i) - PSNR(i, Q_F) & if\ Q_F = 100 \end{cases} \quad (4.6)$$

where, $i = 1, 2, \cdots, 10$ and

$$PSNR(i) = psnr(I_i^w(K), I_i^w(K)) \quad (4.7)$$

As mentioned before, the block with the largest quality gradient is the one whose quantization parameter has the largest effect on changing the vulnerability of the watermark. Thus, by finding the maximum gradient under each quality factor, we can find the quantization parameter that needs to be adjusted under the corresponding image quality degradation.

(e) Find the most contributing block by finding the largest quality gradient.

$$\begin{cases} G(Q_F) = \max\{G(i, Q_F)\} \\ \\ Block(Q_F) = i \end{cases} \tag{4.8}$$

where, $Block(Q_F)$ is the block with the largest quality gradient under one quality factor, Q_F.

(f) To strengthen the adjustment effect, we adjust the quantization parameter(s) of the block(s) in the same DWT level, m. The $1, 2, \cdots, 10$ at the rightmost of the following equation are the block numbers shown in Fig. 4.6.

$$m(Q_F) = \begin{cases} 1 \;\; if \;\; Block(Q_F) \in \{8, 9, 10\} \\ 2 \;\; if \;\; Block(Q_F) \in \{5, 6, 7\} \\ 3 \;\; if \;\; Block(Q_F) \in \{2, 3, 4\} \\ 0 \;\; if \;\; Block(Q_F) = 1 \end{cases} \tag{4.9}$$

For example, if $Block(Q_F)$ belongs to the 1^{st} DWT level, we adjust the quantization parameters of block 8, 9, and 10 at the same time due to their similar contributions to quality degradation of the image.

(g) Find the most frequently appeared DWT level, M, from $m(Q_F)$, where $Q_F = \{100, 90, \cdots, 20\}$.

(h) Find the maximum quality difference associated with level M, $\Delta Quality$ from $\Delta Quality(Q_F)$.

(i) Estimate the increment(s) or decrement(s), $\Delta Quan_M$, for the quantization

parameter(s) of the block(s) of level M.

$$\Delta Quan_M = f(\Delta Quality) = \begin{cases} 10 & \Delta Quality > 2 \\ 5 & 2 \geq \Delta Quality \geq 1.5 \\ 3 & 1.5 \geq \Delta Quality \geq 1 \\ 1 & 1 > \Delta Quality \geq 0.3 \\ 0 & -0.3 < \Delta Quality < 0.3 \\ -1 & -1 < \Delta Quality \leq -0.3 \\ -3 & -1.5 \leq \Delta Quality \leq -1 \\ -5 & -2 \leq \Delta Quality < -1.5 \\ -10 & \Delta Quality < -2 \end{cases} \tag{4.10}$$

(j) Calculate the adjusted quantization parameter(s) of level M.

$$Q'_M = Q_M + \Delta Quan_M \tag{4.11}$$

(k) Output the adjusted quantization parameters, Q', for the 10 DWT decomposed blocks.

$$Q' = [\cdots, Q'_M, \cdots] \tag{4.12}$$

Among the steps summarized above, from step 2(a) to step 2(e) are the processing steps of the gradient calculator.

The quantization parameters are adjusted by simultaneously reducing the quality differences under all the quality factors from 100 to 20 with step -10. Therefore, the result accuracy will not be affected when users estimate image/video quality under

different quality factors.

A detailed example for quantization parameter adjustment is depicted in the following. The data used in the example are tested on a normal textured image under quality factor from 90 to 20 with step -10.

1. Table 4.1 shows the calculated quality differences for one watermarked image with quality factor varying from 90 to 20 with a step of -10.

Table 4.1: The calculated quality differences under different quality factors

Q_F	90	80	70	60	50	40	30	20
$\Delta Quality$	-0.2673	-2.4074	-3.1388	-2.7999	-1.4532	-0.8448	0.0223	0.4211

2. Tabel 4.2 shows the calculated quality gradients for the 10 DWT blocks under different quality factors. The numbers 1 to 10 are the block numbers.

Table 4.2: The calculated quality gradients for the 10 DWT decomposed blocks under different quality factors

Q_F	90	80	70	60	50	40	30	20
1	3.2411	3.7965	3.8884	2.2642	1.8347	1.8186	2.6010	3.3012
2	3.3771	4.4441	2.5165	2.4491	1.2524	1.6267	2.1855	3.0380
3	5.8649	4.7116	2.6989	1.8233	1.1238	1.4413	1.6910	2.4396
4	3.6585	3.8673	3.3079	1.7143	1.4546	1.5295	1.8602	3.1328
5	10.3503	5.1943	2.6815	2.0416	1.5784	1.5834	1.7308	2.6123
6	14.9972	4.9070	2.4197	1.7498	1.2745	1.1276	1.3786	1.8196
7	9.4622	4.9543	2.7476	1.6080	1.4498	1.2664	1.4604	2.1367
8	21.3105	4.8677	2.4376	1.6288	1.1029	1.0516	1.1405	1.3020
9	24.0285	4.0573	1.6812	0.8975	0.5485	0.4315	0.3610	0.3249
10	20.6010	4.7498	2.3002	1.3719	0.9521	0.8311	0.8850	1.0333

3. From Table 4.2, under each distortion, we can find the most contributing block, $Block(Q_F)$, by finding the maximum contribution.

Table 4.3: The most contributing blocks under different quality factors

Q_F	90	80	70	60	50	40	30	20
$Block(Q_F)$	9	5	1	2	1	1	1	1

4. The DWT levels of the most contributing blocks are as following. And the most frequently appeared level is Level 0. Therefore, the quantization parameter of block 1 in level 0 will be adjusted according to the largest quality difference associated with Level 0 which is -3.1388.

Table 4.4: The DWT level of the most contributing blocks under different quality factors

Q_F	90	80	70	60	50	40	30	20
$m(Q_F)$	1	2	0	3	0	0	0	0

5. Combining Table 4.1 and Table 4.4, the quantization parameter will be adjusted as:

$$Q_1' = Q_1 + f(-3.1388) \tag{4.13}$$

4.3 Watermark extraction and quality estimation scheme

Fig. 4.12 shows us the proposed watermark extraction and quality estimation scheme. At the receiver side, the degraded watermark will be directly extracted using the transmitted quantization parameters. The TDR is calculated between the original watermark and the degraded watermark. And the quality is estimated by mapping TDR to PSNR, wPSNR or JND according to the ideal mapping curves.

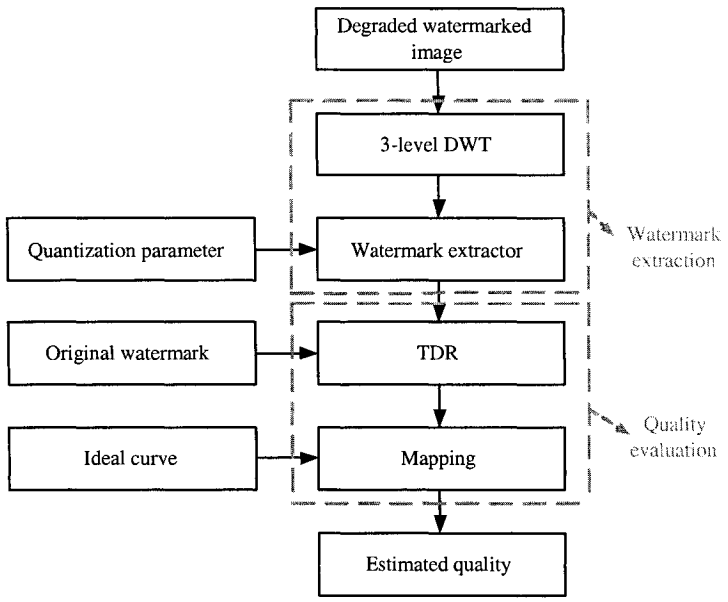

Figure 4.12: The proposed watermark extraction and quality measurement scheme

4.3.1 Decision of 0 or 1 in watermark extraction

As mentioned in Section 4.2, each watermark bit is embedded into 50 selected DWT coefficients. When extracting a watermark bit from the 50 degraded DWT coefficients, $Q(e)$ associated with them will be first calculated using Equ. (4.1). Because the current DWT coefficients of the distorted image might be changed during transmission, the newly calculated $Q(e)$ might be different from those calculated using the coefficients of the original image. The following shows how we extract watermark:

1. If the number of 1 is 8 more than the number of 0, the watermark bit will be detected as 1.

2. If the number of 0 is 8 more than that of 1, the watermark bit will be detected as 0.

3. Otherwise, the watermark bit will be detected as 2 which indicates an error bit.

And the TDR is calculated using Equ. (4.14).

4.4 Watermarking-based quality measurement

To evaluate the quality of the degraded image, we first calculate the True Detection Rates (TDR) of the extracted watermark using Equ. (4.14).

$$TDR = \frac{Number\ of\ correctly\ detected\ watermark\ bits}{Total\ number\ of\ watermark\ bits} \tag{4.14}$$

Through experiments, we found that with the increasing of compression ratios, the TDRs decrease monotonously [7]. Therefore, the quality of the degraded image can be estimated by mapping the calculated TDR to quality in terms of PSNR, or wPSNR, or JND using the empirical ideal curve. Three ideal mapping curves are defined which are respectively for estimating PSNR, wPSNR, and Watson JND.

4.4.1 Ideal mapping curve

The ideal curve is the pre-calculated relationship between the TDR values calculated after the watermark extraction and the quality values calculated with the standard quality metrics, such as PSNR, wPSNR, and JND. Each ideal curve is generated by testing 20 different textured images using only feedforward control.

Fig. 4.13 shows how we generate the ideal curve for estimating PSNR from a set of tested data. In the figure, the 20 curves show the resulting PSNR-TDR relationship for testing 20 different images. On each PSNR-TDR curve, there are 9 points indicating the PSNR values of one image which is compressed with quality factors from 100 to 20 with a step of 10. The ideal curve is composed of the set of big stars. It is generated

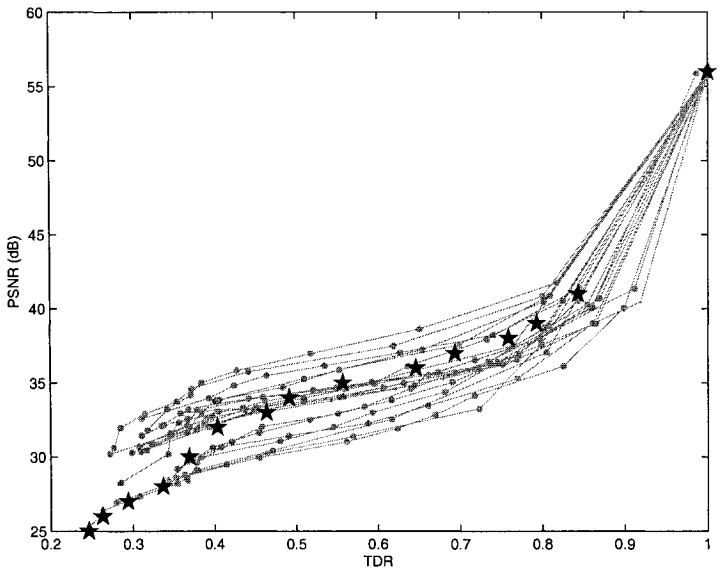

Figure 4.13: Ideal curve generation

by averaging the resulting PSNR values of the 20 images as depicted in Equ. (4.15).

$$V_{Ideal} = \frac{\sum(V_{PSNR})}{N} \qquad V_{PSNR} \in (i, i+1] \tag{4.15}$$

where, $i = \{59, 58, \cdots, 21, 20\}$ and are the possible PSNR values for evaluating the quality of compressed images. V_{PSNR} is the PSNR value of the point on the lines in Fig. 4.13. N is an integer indicating the times when V_{PSNR} locates between i and $i+1$.

The ideal curve is used as the reference for the automatic adjustment of the quantization parameters. Once the tested PSNR-TDR curve of any image is adjusted to converge to the ideal curve, the image quality after compression with an arbitrary quality factor can be estimated with high accuracy by checking PSNR using the ideal curve and the computed TDR.

The principle behind the adjustment is shown as Fig. 4.14. Suppose that from a set of test images, the ideal curve is summarized as shown in Fig. 4.14. For one image,

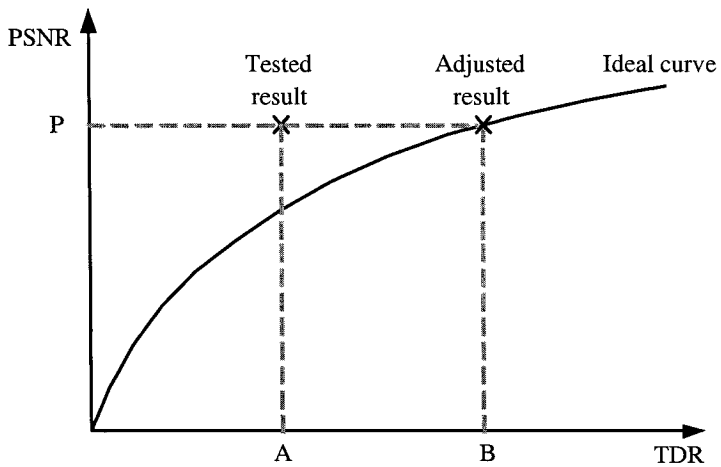

Figure 4.14: The principle of automatic adjustment

under some distortion, we test both the PSNR and TDR. The tested PSNR value is P and the corresponding TDR value is A. The process of adjustment is to adjust the vulnerability of the watermark in order to converge the tested result to the adjusted result. In this case, we need to adjusted the TDR value from A to B so that the PSNR value can be accurately estimated. So during the watermark extraction at the receiver side, the TDR value computed from the extracted watermark is B, then we can make an accurate PSNR estimation from the ideal curve. And the estimated PSNR will be P.

In the following, a complete explanation of the adjustment using feedforward control and feedback control is given. The adjustment process is as: first, we apply the feedforward control. The main method is to assign a certain amount of watermark bit for each wavelet block. The reason of doing so is that: different wavelet block has different frequency distribution, thus we can embed different watermark bits into different wavelet block with different vulnerability. The more watermark bits are embedded; the stronger the watermark embedding strength. In other words, we want to make it possi-

ble that the PSNR-TDR (could be wPSNR-TDR, or JND-TDR) relationship curve of any arbitrary test image under compression falls into the region between upper bound and lower bound. This makes the following feedback adjustment easier. The upper bound curve, lower bound curve and the ideal curve are shown on Fig. 4.15.

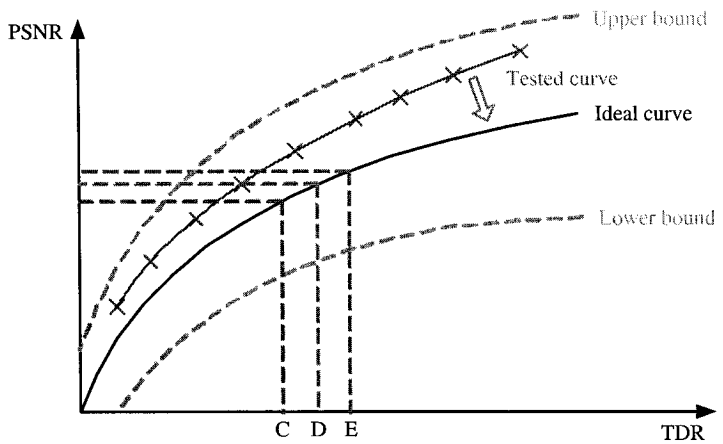

Figure 4.15: An example of automatic adjustment

An example is also shown in Fig. 4.15. The 'Tested curve' is the PSNR-TDR curve of the test image. And those $\times$ symbols on the 'Tested curve' are the tested results. Here, we only executed the test under 9 different quality factors (from 100 to 20 with a step of 10) to get the PSNR-TDR relationship of the test image. These symbols are like sample points on the curve. Obviously, if we execute the test with more quality factors, such as 100 to 20 with a step of 5, we will have more sample points (18 instead of 9). However, from our experiments, we found 9 steps are accurate enough to summarize the ideal curve under compression, and are also good for the speed of convergence.

After the feedforward control, we then use the feedback control to finely adjust the tested PSNR-TDR curve to make it converge to the ideal curve. As shown in Fig. 4.15, we want to make the 'Tested curve' converge to the ideal curve. How to do this

is to adjust the quantization parameters for some of the DWT decomposed blocks. Different wavelet block has different sensitivity to the compression due to its frequency distribution. Thus by adjusting the quantization parameters, we can change the shape of the tested PSNR-TDR curve to make it converge to ideal curve. Detail steps of the quantization step adjustment are given in Section 4.2.3.

At the receiver side, after the watermark extraction, the computed TDR value could lie between two consequent points on the ideal curve, because we could compress the image with arbitrary quality factor. For example, the computed TDR of the test image is D, and the two consequent points on the ideal curve have TDR values C and E. In this case, we use bilinear interpolation to estimate the PSNR using the computed TDR as shown in Fig. 4.15. and in the Section 4.4.2.

The advantage of the ideal curve is that it is the statistical mean and makes the automatic adjustment easier. Because the mean satisfies the requirement of the MMSE (Minimum Mean Square Error), given any tested PSNR-TDR curve, the ideal curve (mean values) should be able to make the needed adjustment less.

In this section, the idea of generating ideal curve and the advantage of it are discussed. Moreover, the automatic control can make the tested PSNR-TDR curve of an image converge to any reasonably pre-defined ideal curve. That means that the ideal curve acts as the role of reference and makes the convergence process easier.

4.4.2 Quality estimation using mapping

"Mapping" in Fig. 4.5 is to map the calculated TDR to PSNR, wPSNR, or JND quality by checking the ideal curve. After watermark extraction, the calculated TDR value could possibly lie between two neighboring TDR values on the ideal curve. In this case, bilinear interpolation is used to estimate quality based on the calculated TDR

value.

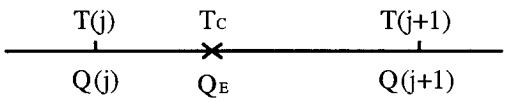

Figure 4.16: Bilinear interpolation

In Fig. 4.16, $(T(j), Q(j))$ and $(T(j+1), Q(j+1))$ are two consequent points on the ideal curve, where T is the TDR and Q is the quality in terms of PSNR, wPSNR, or Watson JND. T_C is the tested TDR of any image under any compression. And Q_E is the estimated quality which can be obtained using Equ. (4.16).

$$Q_E = Q(j) + \frac{T_C - T(j)}{|T(j+1) - T(j)|} \times |Q(j+1) - Q(j)| \tag{4.16}$$

In Chapter 3 and Chapter 4, we introduced the idea and implementation of estimating video/image quality using the watermarking technique. At the receiver side, the proposed scheme can be used to estimate video/image quality without the need for the original work. Through experiments, we found that the watermarking-based quality estimation scheme can work with high accuracy.

Chapter 5

Experimental results

In this chapter, three sets of experimental results are presented. Those are estimating quality respectively in terms of PSNR, wPSNR, and Watson JND. With the proposed watermarking-based quality estimation scheme, the image/video quality can be evaluated at the receiver side without the need for the original work. From the experimental results, we will find that the proposed scheme works with high accuracy.

For each experiment, 25 different textured images were tested under compression with quality factors from 100 to 20 with a step of 10. Therefore, a total of 225 qualities were tested in each experiment.

(a) The original watermark (b) The scrambled watermark

Figure 5.1: The 32×32 original watermark

Fig. 5.1 (a) is the original watermark used in the experiments. It is 32×32. For the

purpose of security, the watermark was scrambled and shown as Fig. 5.1 (b).

And as mentioned in Chapter 4, the watermark portions, [0.0479, 0.25, 0.0195], and the quantization parameters, 80 for all the 10 blocks, were used to embed the watermark.

5.1 Quality measurement in terms of PSNR

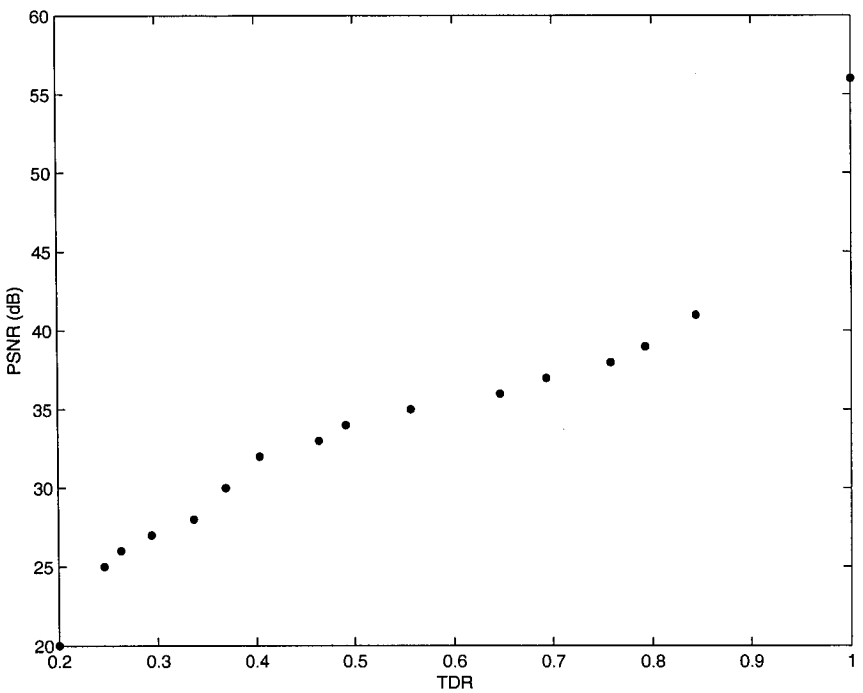

Figure 5.2: The ideal curve used for estimating PSNR

Fig. 5.2 is the ideal curve used for estimating quality in terms of PSNR. This figure shows that the TDR values decrease monotonously with the decrease of PSNR values. Normally, with the decreasing of the quality factor, the image/video quality degrades, and the calculated TDR decreases.

In the following, an example experiment of estimating quality in terms of PSNR, which was tested on Fig. 5.3, is first addressed. The image was compressed with quality factors from 100 to 20 with a step of 10. And the quality of the degraded image was both estimated using the proposed scheme and calculated using the PSNR metric. Fig.

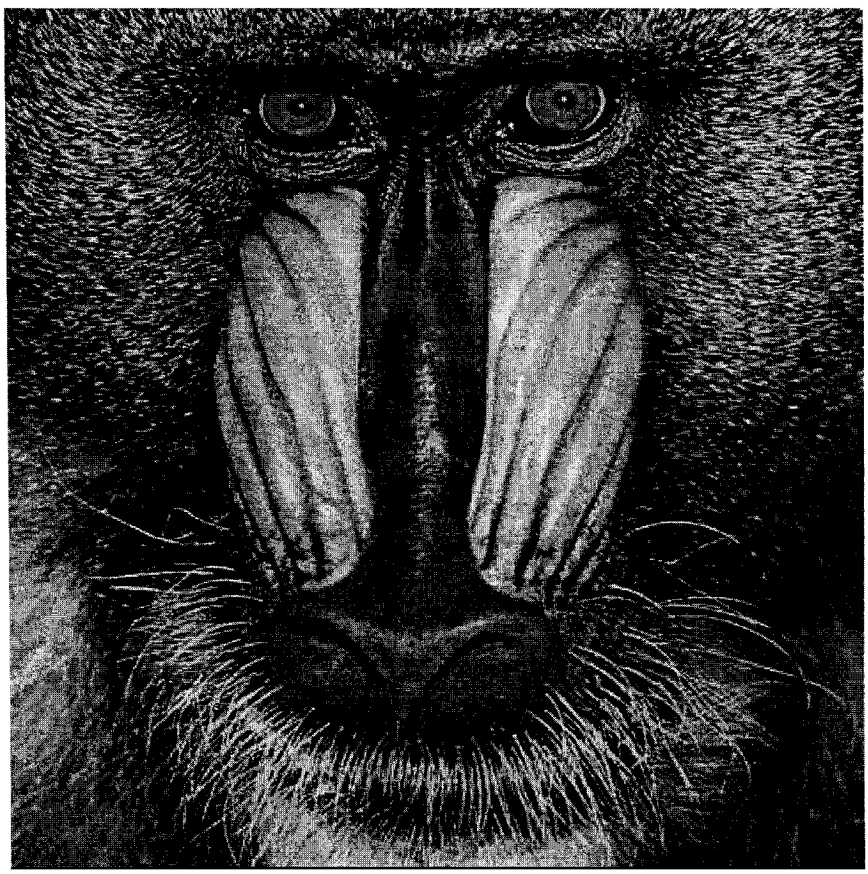

Figure 5.3: The original image Baboon

5.4 shows two sets of experimental results tested on image Baboon. Fig. 5.4 (a) is the result computed without the quantization parameter adjustment. In other words, these results are obtained only with the feedforward control. And Fig. 5.4 (b) is the result acquired with quantization parameter adjustment. That is, they are obtained

with both the feedforward control and the feedback control.

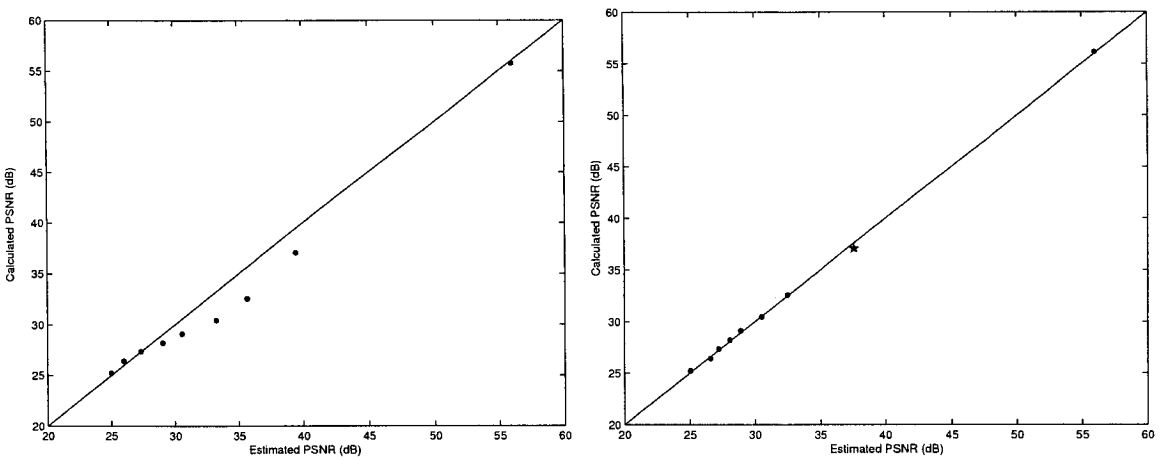

(a) PSNR correlations without quantization parameter adjustment

(b) PSNR correlations with quantization parameter adjustment

Figure 5.4: Correlations between the evaluated PSNR and the calculated PSNR for image Baboon

The x axis is the estimated quality which was obtained using the proposed watermarking-based quality estimation scheme. The y axis is the calculated quality which was computed using the PSNR metric. The solid line in the figure is the match line which indicates that the estimated PSNR equals to the calculated PSNR. The points show the values of both the estimated PSNR and the calculated PSNR. Moreover, they also indicate the relationship between the estimated PSNR and the calculated PSNR. Table 5.1 shows the quality differences, $\Delta Quality$, respectively for the two sets of results in Fig. 5.4, which were calculated using Equ. (4.2).

Table 5.1: Quality differences of the results in Fig. 5.4

Quality factor	100	90	80	70	60	50	40	30	20
$\Delta Quality$ without adjustment	-0.2673	-2.4074	-3.1074	-2.7999	-1.4532	-0.8448	0.0223	0.4211	0.2074
$\Delta Quality$ with adjustment	0.1463	-0.5505	0.0953	-0.0595	0.2033	0.1322	0.1230	-0.1748	0.1614

From Table 5.1, we find that the solid line also indicates the accuracy of the quality estimation. The more converged the points to the solid line, the more accurate the quality estimation.

In Fig. 5.4 (b), a point was emphasized using the star, which is the result under compression with the quality factor of 90. For this point, the calculated PSNR is 37.0700 dB, and the estimated PSNR is 37.6205 dB. In this case, the proposed algorithm overestimated 0.5505 dB.

Based on the above analysis, we know, the accuracy of the estimation was much improved with the quantization parameter adjustment. The estimation accuracy was also evaluated using the Mean Absolute Error (MAE) as depicted in Equ. (5.1)

$$MAE = \frac{\sum |\Delta Quality|}{N} = \frac{\sum |Calculated\ Quality - Estimated\ Quality|}{N} \tag{5.1}$$

where, N is the number of qualities tested in the experiment.

For Fig. 5.4 (a), the MAE of the results is 1.2812 dB, and the quantization parameters are [80 80 80 80 80 80 80 80 80 80]. For Fig. 5.4 (b), the MAE of the results is 0.1829 dB, and the adjusted quantization parameters are [80 80 80 80 110 110 110 90 90 90]. Therefore, for Baboon, the accuracy of quality estimation was effectively improved with the quantization parameter adjustment.

We also applied our algorithm to 25 different textured images. And the results are shown in Fig. 5.5. Each image is compressed with quality factors from 100 to 20 with a step of 10. Therefore, a total of 225 qualities are tested. Fig. 5.5 (a) show the results obtained without quantization parameter adjustment. Most of the points scattered away from the solid line. However, we can find, at the upper-right corner, all the points are exactly on the solid line. That is because those points are tested with the quality

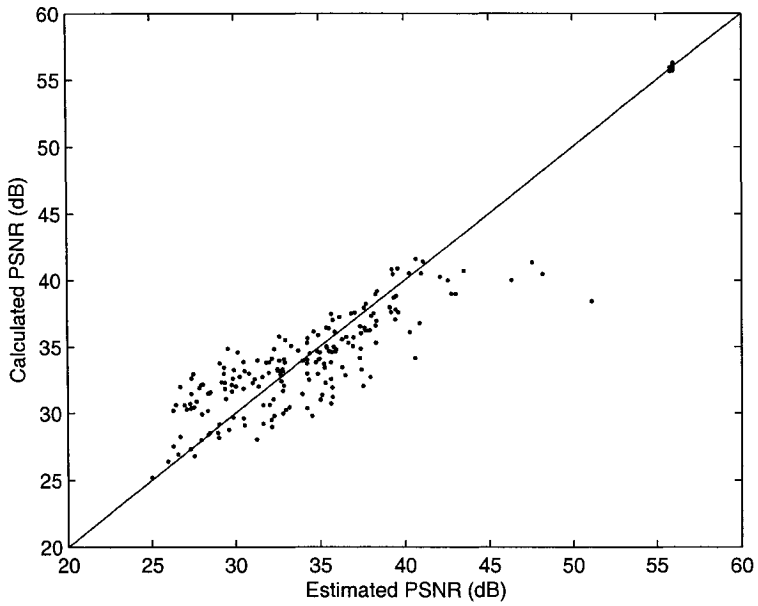

(a) PSNR correlations without quantization parameter adjustment (MAE=2.2330 dB)

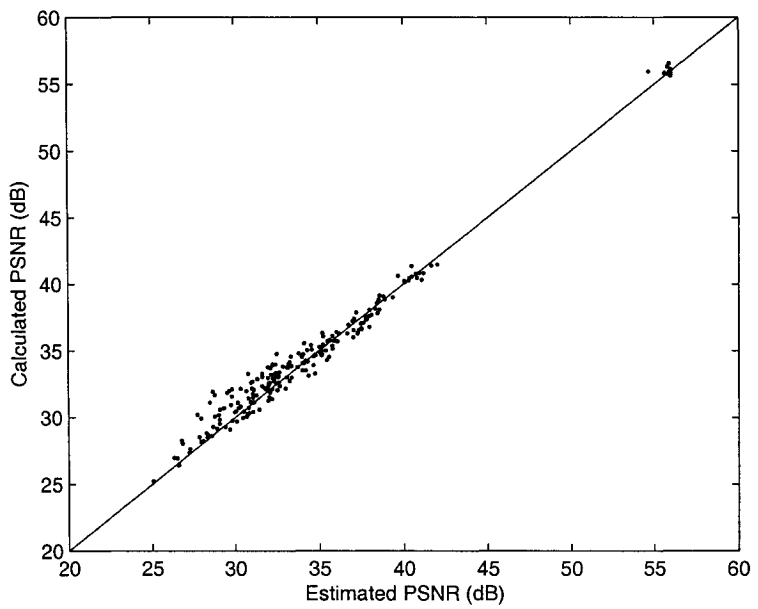

(b) PSNR correlations with quantization parameter adjustment (MAE=0.6363 dB)

Figure 5.5: Correlations between the evaluated PSNR and the calculated PSNR

factor of 100. All the quality degradations are only caused by the format change. In this case, with the redundancy of watermark embedding (refer to Section 4.2.1), the watermark can be extracted without any errors.

Fig. 5.5 (b) is the result obtained with quantization parameter adjustment. All the points are much converged to the solid line. Normally the larger the JPEG quality factor, the better the image quality after compression. Consequently, the calculated PSNR will be larger. So it can be seen in Fig. 5.5 (b) that with the decreasing of JPEG quality factors, these points are more scattered. This is because the accuracy of the quality estimation decreases as the image quality deteriorates severely when compressed using a very small JPEG quality factor.

The MAE of the results in Fig. 5.5 (a) is 2.2330 dB. And the MAE of the results in Fig. 5.5 (b) is 0.6363 dB, which means, by employing the watermarking-based quality estimation scheme, the PSNR of the images can be estimated only with an error of 0.6363 dB.

From both the figure and the calculated MAE values, we can conclude that the accuracy of estimating quality in terms of PSNR is effectively improved with the quantization parameter adjustment. And the PSNR of image/video can be accurately estimated at the receiver side without the need for the original work.

5.2 Quality measurement in terms of wPSNR

Fig. 5.6 is the ideal curve used to map the calculated TDR to the quality in terms of wPSNR. It is similar to Fig. 5.2. With the decreasing of the JPEG quality factor, the image quality degrades. Therefore, the wPSNR values decrease and the calculated TDRs decrease monotonously with wPSNR.

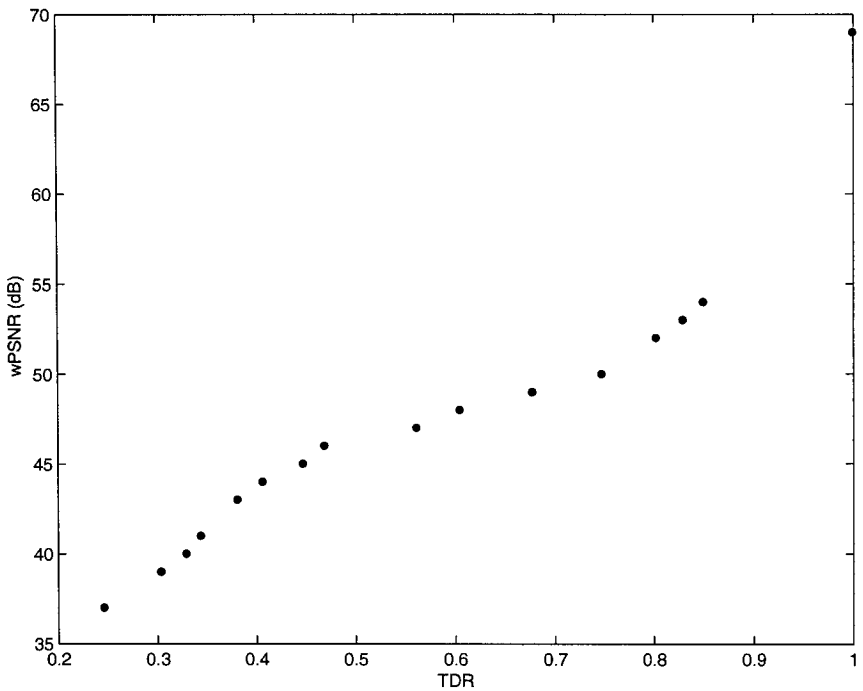

Figure 5.6: The ideal curve used for estimating wPSNR

Fig. 5.7 shows the results of estimating quality in terms of wPSNR. Fig. 5.7 (a) is the experimental result obtained without the quantization parameter adjustment. Similar to Fig. 5.5 (a), most of the points scatter away from the solid line. Fig. 5.7 (b) is the result obtained with quantization parameter adjustment. We can see that, with the quantization parameter adjustment, all the points are much converged to the solid line. The points whose wPSNR values are smaller than 45 dB are a little more scattered than the other points, because the image quality under these conditions is more severely damaged than the image quality under other conditions.

The calculated MAE of the results in Fig. 5.6 (a) is 1.9651 dB. And the MAE of the results in Fig. 5.6 (b) is 0.6310 dB. Both the figure and the calculated MAE indicate that the accuracy of estimating quality in terms of wPSNR is greatly improved.

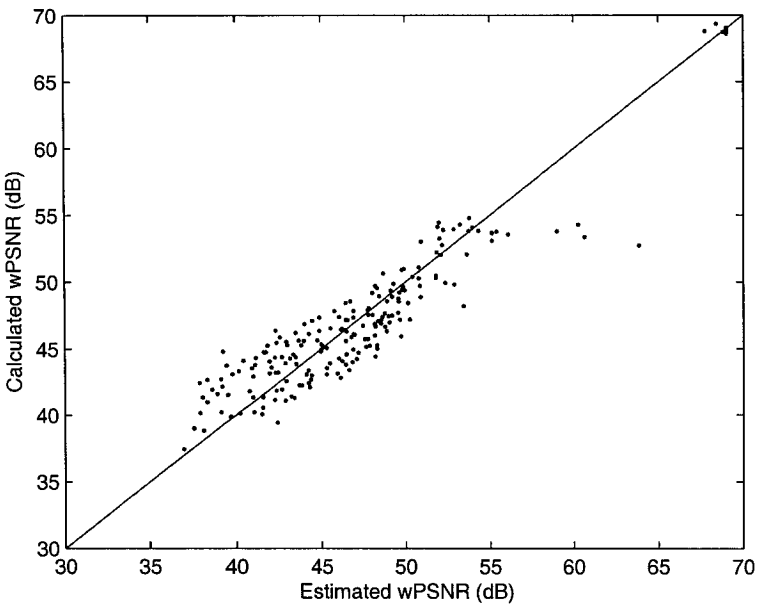

(a) wPSNR correlations without quantization parameter adjustment (MAE=1.9651 dB)

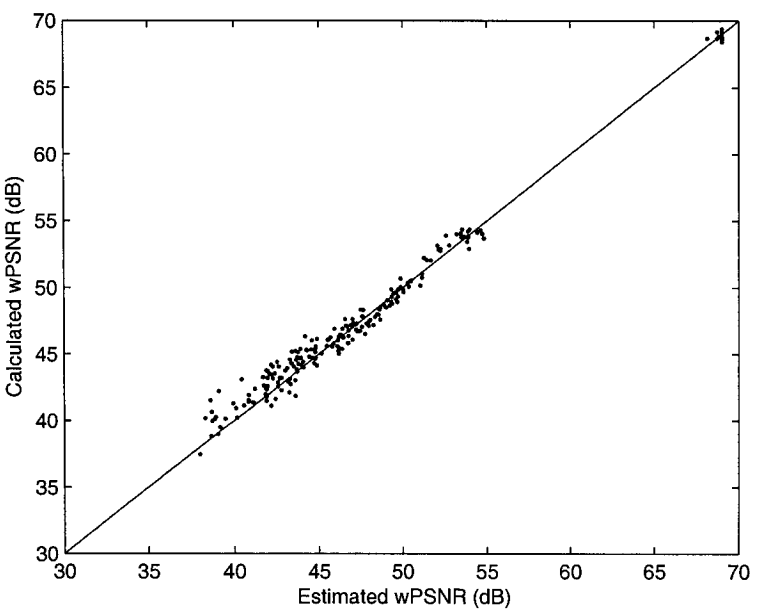

(b) wPSNR correlations with quantization parameter adjustment (MAE=0.6310 dB)

Figure 5.7: Correlations between the evaluated wPSNR and the calculated wPSNR

5.3 Quality measurement in terms of JND

The proposed watermarking-based quality estimation scheme can also be used to estimate quality in terms of JND. In the experiment, the JND based on the Watson model was used for estimation. The software Dctune2.0 [47] is used to calculate the JND.

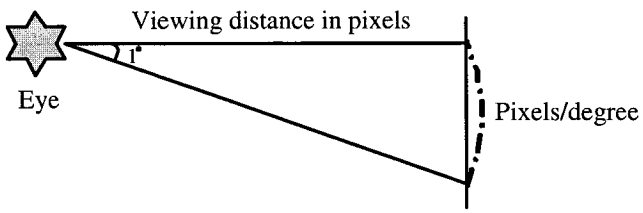

Figure 5.8: The default parameters of Dctune2.0

The default parameters of Dctune2.0 shown in Fig. 5.8 are:

1. The resolution of the computer is defaulted as the standard screen resolution 72 dpi.

2. Both the horizontal and vertical pixels density are 32 pixels/degree.

3. The viewing distance from the human eye to the screen is calculated as 25.333 inches.

Fig. 5.9 is the ideal curve used for estimating quality in terms of JND. With the decreasing of the JPEG quality factor, the image quality degrades. Therefore, the JND values increase, while the calculated TDRs decrease.

Fig. 5.10 shows the result of estimating JND. Fig. 5.10 (a) is the result obtained without the quantization parameter adjustment. The points in this figure scatter away from the solid line. Meanwhile, with the increasing of the JND values, the points are more scattered due to the more severe damages to the images. Fig. 5.10 (b) is the result

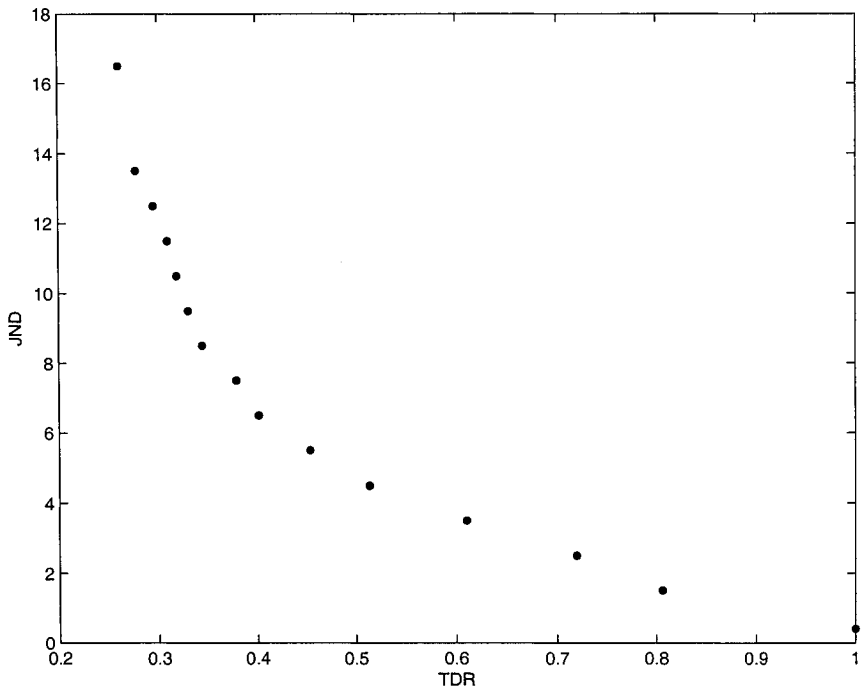

Figure 5.9: The ideal curve used for estimating JND

obtained with the quantization parameter adjustment. The points are much converged to the solid line. The MAE of the results in Fig. 5.10 (a) is 1.5146 JND. And the MAE of the results in Fig. 5.10 (b) is 0.4509 JND. The estimation accuracy is effectively improved. Thus, we can estimate quality in terms of JND only with an error of 0.4509 JND.

On the other hand, in Fig. 5.10 (b), the points become more scattered when the JND value is greater than 8. This is due to the fact that the JPEG quality factor is smaller than about 30 and the resulting image and the watermark are severely damaged. However, when the JND is bigger than 8 (or when the JPEG quality factor is smaller than 30), the image begins to lose its value. For the points whose JND values are less than or equal to 8 in Fig. 5.10 (b), the MAE is 0.2975 JND.

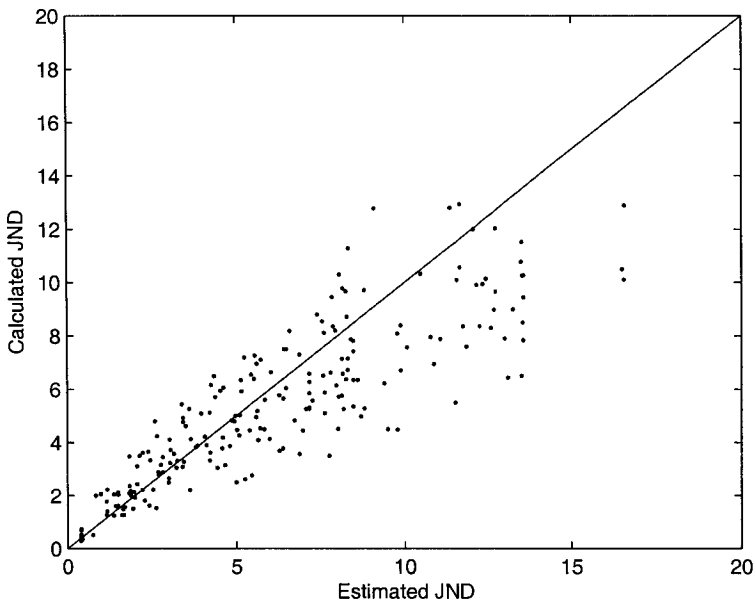

(a) JND correlations without quantization parameter adjustment (MAE=1.5146 JND)

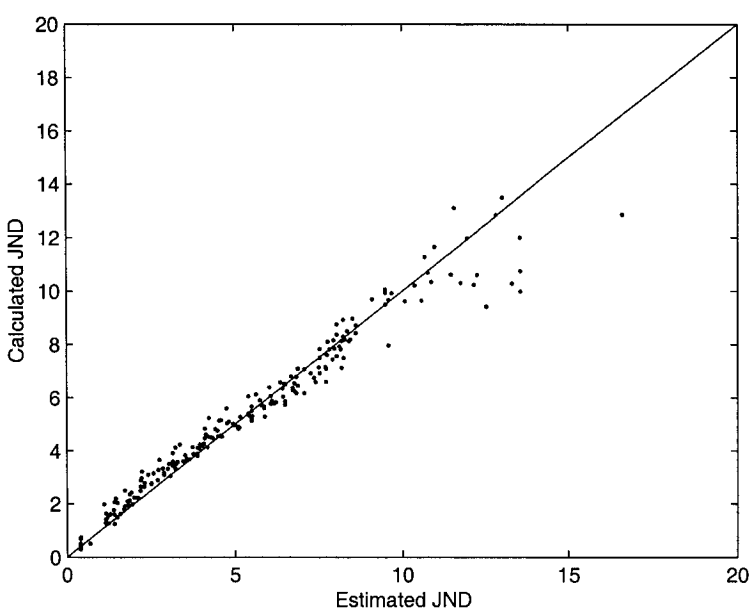

(a) JND correlations with quantization parameter adjustment (MAE=0.4509 JND)

Figure 5.10: Correlations between the evaluated JND and the calculated JND

In this chapter, the experimental results of estimating quality in terms of PSNR, wPSNR, and Watson JND are presented. And from both the figures and the analysis, we can conclude the automatic control is very effective to be used to improve the accuracy of quality estimation. By employing the automatic control, the errors of estimating image image/video quality in terms of PSNR, wPSNR, and JND are respectively 0.6363 dB, 0.6310 dB, and 0.4509 JND. Therefore, at the receiver side, we can accurately estimate image/video quality without the need for the original work. Meanwhile, by employing a different ideal mapping curve, the proposed method can be used to evaluate image quality in terms of other quality metrics.

Chapter 6

Conclusions and future work

This thesis presented a method of objective video quality measurement. The watermark is embedded by quantizing the DWT coefficients of the original I-frame and the degradation of the watermark can reflect the degradation of the video quality. To improve the accuracy of quality estimation, the watermark vulnerability was automatically adjusted according to the different frequency distribution of the cover work. Therefore, the TDR computed using the original watermark and the degraded watermark can be used to estimate the image/video quality in terms of PSNR, wPSNR and Watson model. The evaluations demonstrated the effectiveness of the proposed scheme against compression. And we can use this watermarking based quality metric to estimate image/video quality without the access to the original image/video.

Meanwhile, the proposed scheme can also be used to select the suitable video frames/images for watermark embedding. Considering the characteristics of JPEG/MPEG compression, the watermarking based metric can more accurately track the existing quality metrics such as PSNR, wPSNR and Watson model when the video frames/images have relatively rich textures and details. Broader frequency distribu-

tion and richer detail means more information can be used for quantization parameter adjustment.

As for the future work, more perceptual features proposed in the original-work-dependent algorithms can be utilized such as local distortion, cross-block weighting. If necessary, other techniques such as edge detection and image segmentation can be used to determine the suitable watermark embedding locations. More advanced perceptual models will be examined and more meaningful watermark pattern will be used.

Bibliography

[1] Y.-C. Chen and L.-W. Chang, "A secure and robust digital watermarking technique by the block cipher RC6 and secure hash algorithm," *Proc. of IEEE International Conference on Image Processing,* pp. 518–521, Vol. 2, Oct. 2001.

[2] I.J. Cox, J. Kilian, F.T. Leighton, and T. Shamoon, "Secure spread spectrum watermarking for multimedia," *IEEE Transactions on Image Processing,* pp. 1673–1687, Vol. 6, Issue 12, Dec. 1997.

[3] Y. Wang, J.F. Doherty, and R.E. Van Dyck, "A wavelet-based watermarking algorithm for ownership verification of digital images," *IEEE Transactions on Image Processing,* pp. 77–88, Vol. 11, Issue 2, Feb. 2002.

[4] M. Wu and B. Liu, "Watermarking for image authentication," *Proc. of IEEE International Conference on Image Processing,* pp. 437–441, Vol. 2, Oct. 1998.

[5] O. Ekici, B. Coskun, U. Naci, and B. Sankur, "Comparative assessment of semi-Fragile watermarking techniques," *Proc. of SPIE, Multimedia Systems and Applications IV,* pp.177-188, Vol. 4518, Aug. 2001.

[6] S. Wang, D. Zheng, J. Zhao, W.J. Tam, and F. Speranza, "A Digital Watermarking

and Perceptual Model Based Video Quality Measurement," *Proc. of IEEE Instrumentation and Measurement Technology Conference,* pp.1729-1734, May 2005.

[7] S. Wang, J. Zhao, W.J. Tam, and F. Speranza, "Image quality measurement by using digital watermarking based on discrete wavelet transform," *Proc. of the 22nd Biennial Symposium on Communications,* pp. 210–212, Jun. 2004.

[8] A.B. Watson, J. Hu, and J.f. McGowan, "DVQ: A digital video quality based on human vision," *Journal of Electronic Imaging,* pp. 20–29, Vol. 10, Issue 1, Jan. 2001.

[9] S. Wang, D. Zheng, J. Zhao, W.J. Tam, and F. Speranza, "Video quality measurement using digital watermarking," *Proc. of IEEE International Workshop on Haptic, Audio and Visual Environments and Their Applications,* pp. 183-188, Oct. 2004.

[10] D. Zheng, J. Zhao, W.J. Tam, and F. Speranza, "Image quality measurement by using digital watermarking," *Proc. of IEEE International Workshop on Haptic, Audio and Visual Environments and Their Applications,* pp. 65–70, Sept. 2003.

[11] R. Tu and J. Zhao, "A novel semi-fragile audio watermarking scheme," *Proc. of IEEE International Workshop on Haptic, Audio and Visual Environments and Their Applications,* pp. 89–94, Sept. 2003.

[12] "Objective picture quality measurement method by use of in-service test signals", *ITU-T J.147,* Jul. 2002.

[13] M. Holliman and M. Young, "Watermarking for automatic quality monitoring,"

Proc. of SPIE, Security and Watermarking of Multimedia Contents IV, pp. 458-469, Vol. 4675, Jan. 2002.

[14] P. Campisi, M. Carli, G. Giunta, and A. Neri, "Blind Quality Assessment System for Multimedia Communications Using Tracing Watermarking," *IEEE Transactions on Signal Processing,* pp. 996-1002, Vol. 51, Issue 4, Apr. 2003.

[15] F. Hartung and B. Girod, "Watermarking of uncompressed and compressed video," *Singal Processing*, pp. 283-301, Vol. 66, Issue 3, May 1998.

[16] S. Bossi, F. Mapelli, and R. Lancini, "Objective video quality evaluation by using semi-fragile watermarking," *Proc. of Picture Coding Symposium (PCS2004),* Dec. 2004.

[17] O. Sugimoto, R. Kawada, M. Wada, and S. Matsumoto, "Objective measurement scheme for perceived picture quality degradation caused by MPEG encoding without any reference pictures," *Proc. of SPIE, Visual Communications and Image Processing,* pp. 932-939, Vol. 4310, Jan. 2001.

[18] S. Saviotti, F. Mapelli, and R. Lancini, "Video quality analysis using a watermarking technique," *5th International Workshop on Image Analysis for Multimedia Interactive Services (WIAMIS2004),* Apr. 2004.

[19] M.C.Q. Farias, S.K. Mitra, and M. Carli "Video quality objective metric using data hiding," *Proc. of IEEE Workshop on Multimedia Signal Processing (MMSP),* pp. 424-427, Dec. 2002.

[20] Z. Wang, H.R. Sheikh, and A.C. Bovik, "Objective video quality assessment,"

Handbook of Video Databases: Design and Applications, CRC Press, pp. 1041-1078, 2003.

[21] J. Watkinson, "MPEG-2", *Focal Press*, 1999, ISBN 0240515102.

[22] M. Miyahara, K. Kotani, and V.R. Algazi, "Objective picture quality scale (PQS) for image coding," *IEEE Transactions on Communications,* pp. 1215-1226, Vol. 46, Issue 9, Sept. 1998.

[23] *http://www.uottawa.ca/help/about/graphic_stds.html*, last visited on Jun. 01, 2004.

[24] I. Cox, M. Miller, and J. Bloom, "Digital Watermarking," *Morgan Kaufmann*, 2002, ISBN 1558607145.

[25] P.-W. Chan and M.R. Lyu, "A DWT-based digital video watermarking scheme with error correcting code," *Proc. of Fifth International Conference on Information and Communications Security (ICICS2003),* pp. 202-213, Oct. 2003

[26] D. Kundur and D. Hatzinakos, "Digital watermarking for telltale tamper proofing and authentication," *Proc. of the IEEE,* pp. 1167-1179, Vol. 87, Issue 7, Jul. 1999.

[27] D. Kundur and D. Hatzinakos, "A robust digital image watermarking method using wavelet based fusion," *Proc. of IEEE International Conference on Image Processing,* pp. 544-547, Vol. 1, Oct. 1997.

[28] Z. Wang, L. Lu, Bovic A.C, "Video quality assessment using structral distortion measurement," *Proc. of IEEE International Conference on Image Processing,* pp. 65-68, Vol. 3, Jun. 2002.

[29] M.C.Q Farias, M. Carli, A. Neri, and S.K. Mitra, "Video quality assessment based on data hiding driven by optical flow information," *Proc. of SPIE, Image Quality and System Performance,* pp. 190-200, Vol. 5294, Jan. 2004.

[30] P. Campisi, M. Carli, G. Giunta, and A. Neri, "Blind quality assessment system for multimeida communications using tracing watermarking," *IEEE Transactions on Singal Processing,* pp. 996–1002, Vol. 51, Issue 4, Apr. 2003.

[31] S. Winkler, "Visual fidelity and perceived quality: Toward comprehensive metrics," *Proc. SPIE, Human Vision and Electronic Imaging,* pp. 114-125, Vol. 4299, Jan. 2001.

[32] A.J. Ahumada and H.A. Peterson, "Luminance-model-based DCT quantization for color image compression," *Proc. of SPIE, Human Vision, Visual Processing, and Digital Display III,* pp. 365-374, Vol. 1666, Aug. 1992.

[33] P. Campisi, A. Neri, and M. Visconti, "Wavelet-based method for high-frequency subband watermark embedding," *Proc. of SPIE, Multimedia Systems and Applications III,* pp. 344-353, Vol. 4209, Mar. 2001.

[34] N. Narita, "Comparison of subjective evaluation methods using impairments units," *IEEE Transactions on Broadcasting,* pp. 185-191, Vol. 50, Issue 2, Jun. 2004.

[35] N. Narita and Y. Sugiura, "On an absolute evaluation method of the quality of television sequences," *IEEE Transactions on Broadcasting*, pp. 26-35, Vol. 43, Issue 1, Mar. 1997.

[36] J.L. Mannos and D.J. Sakrison, "The effects of a visual fidelity criterion on the

encoding of images," *IEEE Transactions on Information Theory,* pp. 525-536 Vol. 20, Issue 4, Jul. 1974.

[37] F. Bartolini, M. Barni, V. Cappellini, and A. Piva, "Mask building for perceptual hiding frequency embedded watermraks," *Proc. of IEEE International Conference on Image Processing (ICIP '98),* pp. 450-454, Vol. 1, Oct. 1998.

[38] A.B. Watson, "DCT quantization matrices visually optimized for individual images," *Proc. of SPIE, Human Vision, Visual Processing, and Digital Display IV,* pp. 202-216, Vol. 1913, Feb. 1993.

[39] M.C.Q. Farias, S.K. Mitra, M.Carli, and A. Neri, "A comparison between an objective measure and the mean annoyance values of watermarked videos," *Proc. of IEEE International Conference on Image Processing,* pp. 469-472, Vol. 3, 2002.

[40] H. Inoue, A.Miyazaki, and T. Katsura, "An image watermarking method based on the wavelet transform," *Proc. of IEEE International Conference on Image Processing 1999,* pp. 296-300, Vol.1, Oct. 1999.

[41] C.-H. Chang, Z. Ye, and M. Zhang, "Fuzzy-art based adaptive digital watermarking scheme," *IEEE Transactions on Circuits and Systems for Video Technology,* pp. 65-81, Vol. 15, Issue 1, Jan. 2005.

[42] Al Bovik (Editor), "Handbook of image and video processing," *Academic Press,* May 2000, ISBN 0121197905.

[43] D.B. Percival, and A.T. Walden, "Wavelet methods for time series analysis," *Cambridge University Press,* Jul. 2000, ISBN 0521640687.

[44] B.C. Kuo and F. Golnaraghi, "Automatic control system," *John Wiley & Sons Inc.,* Aug. 2002, ISBN 0471134767.

[45] W.A. Wolovich, "Automatic control system: Basic analysis and design," *W. B. Saunders Company,* Jan. 1993, ISBN 0030237734.

[46] F.H. Raven, "Automatic control engineering," *McGraw-Hill Ryerson Limited,* Jan., 1994, ISBN 0070513414.

[47] *http://vision.arc.nasa.gov/dctune/*, last visit on Aug. 25, 2005.